TESTING A MESOPORE AND MATRIX MODEL FOR USE ON SHRINK-SWELL SOILS

A Thesis

by

DIANNA KATHLEEN BAGNALL

Submitted to the Office of Graduate and Professional Studies of
Texas A&M University
in partial fulfillment of the requirements for the degree of

MASTER OF SCIENCE

Chair of Committee,	Cristine L.S. Morgan
Committee Members,	James L. Heilman
	Georgianne W. Moore
Head of Department,	David Baltensperger

December 2014

Major Subject: Soil Science

ABSTRACT

Void space caused by drying of shrink-swell soils forms desiccation cracks and mesopores which conduct water from the soil surface, influencing water redistribution and complicating the partitioning infiltration and runoff. These paths impact hydrology, but often are not included in models because the standard method of modeling flow through soil (Richards' equation) assumes a continuous matrix of particles-this assumption is invalidated by voids, the changing volume of paths is difficult to characterize, and parameters to simulate water flow are difficult to obtain for preferential flow routines. The Precision Agriculture Landscape Modeling System (PALMS) contains a Mesopore and Matrix (M&M) module, which was tested on cracking soil at the plot and field scale.

The M&M module predicted 10 times more mesopore area than, but was linearly related to, measurements of crack area. Four irrigation events on plots of cracked soil and volumetric water content (VWC) output for the M&M module was compared to neutron moisture meter readings. Previous measurements of VWC and runoff on a 4.4 ha subwatershed were compared to predictions. The M&M module moved water down the profile quickly and eliminated unobserved ponding (plot) and runoff (field) that were simulated without the mesopores, modeling mesopore flow did produce more drainage. Simulations of water content of the soil profile were generally improved when the M&M module was used. The M&M module had easily obtainable and physically relevant parameters. The M&M module is a useful tool for model assisted decision making on landscapes where preferential flow occurs.

DEDICATION

To Sybil, Tina, Cristine, and Jessica.

You were real and you were there.

ACKNOWLEDGEMENTS

I would like to thank my committee chair, Dr. C. Lois Morgan, and my committee members, Dr. Heilman and Dr. Moore, for their guidance and support throughout the course of this research. Dr. Morgan has been my chief mentor throughout my college career. Her ability to balance work ethic and grace will continue to benefit my life as it has my education. Christine Molling deserves thanks for contributing her skills and guidance to this work. The staff of the Texas A&M University supercomputing facility (http://sc.tamu.edu/) proved a valuable resource in completing my project.

The Department of Soil and Crop Sciences at Texas A&M University is filled with people who have gone out of their way to ensure the success of my undergraduate and graduate careers. At the Overton Research station, I credit Dr. Vince Haby and Allen Leonard with giving me a foundation in soil science along with their mentorship. Particular thanks go to Dr. David Zuberer and Mark Hall for their advocacy and compassion. Our lab team has been my family since 2010. Dr. Haly Neely, Jason Ackerson, Heather Watson, Chase Vasbinder, Jose Fuentes, James Vandyke, Gregory Rouze, Elizabeth Marley, and Pilar Crespo have all been key parts of that team.

I would like to thank my mother for the love of learning that she shared with me in my young life. Thanks to my grandfather, Ralph Garret Sr., whose love of the land inspired my own. I extend special thanks to my husband Cody for making life better.

DEFINITIONS

Model	A computer based, stand alone, system describing many equations working together, to describe knowledge of biophysical processes.
Module	A component of a model focused on one or a few elements of a system such as a module for soil water flow or plant water uptake.
Crack	A soil preferential flow path that was formed by the desiccation of a shrink-swell soil.
Mesopore	A soil preferential flow path that formed by means other than desiccation, such as biotic activity or soil structural development.
Single-domain flow	Modeling of water flow through a continuous, homogenous matrix of solid particles in response to matric potential.
Two-domain flow	Modeling of water flow through soil using two distinct physical processes. One process assumes a continuous, homogenous matrix of solid particles (Darcy's law) and the other assumes laminar transport through a defined geometry (Poiseuille's law).

TABLE OF CONTENTS

LIST OF FIGURES

LIST OF TABLES

CHAPTER I

INTRODUCTION AND LITERATURE REVIEW

Cracking soils are prevalent in Texas (Fig.1.1). These cracking soils are high clay soils that shrink with water loss and swell when they are wetted. When these soils are dry they may form cracks, some of which are quite large (Fig. 1.2), that will close as the water content of the soil increases. The volume of these desiccation cracks and how that volume changes over time with changes in water content is poorly understood.

Figure. 1.1. Distribution of shrink-swell soils in Texas (USDA-NRCS database).

Figure. 1.2. Desiccation crack in shrink-swell soil near College Station, Texas.

Water flowing through cracks in the soil may bypass portions of the soil matrix and move deeper into the soil profile, even reaching ground water (Greve et al., 2010). This bypassing of the soil matrix by water is termed preferential flow. Preferential flow

impacts agricultural, natural, and urban ecosystems by influencing rainfall redistribution (Novák et al., 2000; Greve et al., 2010), accelerating the contamination of groundwater (Larsson and Jarvis, 1999; Šimůnek et al., 2003), and complicating the partitioning of rainfall between infiltration and runoff (Beven and Germann, 1982; Harmel et al., 2006; Kishné et al., 2010). Modeling water flow through soils with large cracks has essentially been ignored by hydrologists and has been a long-time challenge for soil scientists, as made clear by the statement "soil cracks, as major components in the water transport network, make mathematical analysis of water flow in such soils virtually impossible" (Topp and Davis, 1981). Though difficult, modeling water flow through cracking soils is important for model assisted decision making. Such modeling is useful when making decisions about tillage practices, crop irrigation, flood prediction and urban planning.

There are three challenges in modeling water flow through desiccation cracks. First, the most widely accepted method of characterizing water flow through soil, Richards' equation (Richards,1931), assumes a homogenous media, but a combination of flow through the soil matrix and preferential flow paths invalidates the assumption of homogeneity (Bouma and Dekker, 1978; Beven and Germann, 1982; Wang et al., 1994; Lepore et al., 2009). The second difficulty is that, though a variety of models have been developed to represent flow through heterogeneous media, or multiple pore networks, the parameters required to describe the pore networks are often impractical to obtain for landscape-scale modeling (Novák et al., 2000; Šimůnek et al., 2003; Jarvis, 2008; van Schaik et al., 2010). Thirdly, even if the needed parameters are obtained, desiccation cracks are dynamic and change with soil moisture, that is, a physically-based model

would need to change the size of desiccation cracks as a function of soil moisture (Bouma & Dekker, 1978).

A module that can represent preferential flow through soil with desiccation cracks is needed in hydrology models that will be used in agricultural decision making in the state of Texas (Harmel et al., 2006). The goal of this project is not to create a stand-alone cracking module, but to investigate the performance of a preferential flow module in an existing soil hydrology model. A model that can handle preferential flow of water through soil cracks should have the following characteristics: 1) the ability to represent flow through a heterogeneous system, 2) have practically obtainable parameters at the landscape scale, and 3) allow for dynamic volume of cracks. An existing preferential flow module, the Mesopore and Matrix (M&M) module, will be evaluated for its ability to model water flow in and on a high clay shrink-swell soil with open desiccation cracks.

The M&M module is a component of the Precision Agriculture Landscape Modeling System (PALMS), which is an existing biophysical model used for agricultural decision making. The PALMS M&M module was chosen for this project because it addresses each of the modeling challenges listed above. The M&M module simulates water flow both through the soil matrix and between soil structural units to address the phenomena of preferential flow. The difficulty in obtaining parameters is addressed in the M&M module by using morphological descriptions of soil structure available through the National Resource Conservation Service (National Cooperative Soil Survey, 2014) to characterize the soil system. The dynamic nature of soil cracks might be addressed by using the coefficient of linear extensibility (COLE) to change the

volume that is available for preferential flow with changes in soil water content, but the PALMS M&M module has not been tested on cracking soils. The overall objective of this research project is to test the applicability of the M&M module to handle infiltration and redistribution of water in a high-clay soil that cracks. To do this, studies were conducted to 1) compare the volume of preferential flow paths generated by the PALMS M&M module and another shrinkage model to in-field measurements of crack volume in the same field and on the same soil used for the redistribution measurements (chapter II), 2) understand how the COLE in the M&M module affects preferential flow and redistribution of water (chapter II), and 3) compare field measurements of the redistribution of soil water to PALMS simulations (chapter III).

Preferential Flow in Soils

Modeling of soils as a continuous, homogenous matrix of soil particles has benefits in ease of use and simplicity, but may not apply well to some soils. The rate at which water flows through a continuous soil matrix is governed by the hydraulic conductivity of the media, which is an expression of the ease with which water may move through the soil particles. Soil hydraulic conductivity may be estimated using the particle size distribution of a soil (Rawls et al., 1992). While soils are made up of particles, these particles aggregate to form structure under the influence of soil forming factors (climate, biota, time, parent material, and relief). These aggregates of particles, referred to as peds, collectively form the structure of the soil. The interfaces between peds conduct water down the soil profile, bypassing the soil matrix, therefore this flow is not governed by the soil matrix hydraulic conductivity. Rather, it responds primarily to

gravity and is termed preferential flow. Preferential flow will allow water to move faster down the soil profile because the flow is not restricted by soil particles in its path. Well-structured soils may have many preferential flow paths because of the continuousness and abundance of soil structure interfaces.

Cracking soils of interest in this project change their structure as soil peds shrink and swell, making them challenging to measure and model (Bouma, 1980). When dry, soil peds shrink; opening up larger slits between peds. When dry, these soils also possess massive preferential flow paths in the form of desiccation cracks. When wet, these shrink-swell soils have very low hydraulic conductivities because of their high clay content. It has been established that shrink-swell soils, when dry, allow a great deal of water to infiltrate the soil (Bouma, 1980; Harmel, 2006). It is not clear what the relative contribution of drying soil structural units and soil desiccation cracks may be. Both act as preferential flow paths during rain events and both change volume with changes in soil water content.

Visual inspection shows us that the geometry and volume of desiccations cracks are dynamic. It seems intuitive that correctly characterizing the volume of cracks would improve estimates of water flow and redistribution. For this reason, measuring the volume of cracks in the field has been an aim of many researchers. In-field methods of crack measurements have included physical measurements of depth, width, and length (Kishné et al., 2009), estimation of crack volume based on soil subsidence (Bronswijk, 1989; Arnold et al., 2005), and infilling of the cracks with a material such as wax or sand (Dasog and Shashidhara, 1993; Peng et al., 2006). Measurements of crack depth, width

and length are tedious and time consuming and are also complicated by the self-mulching surface of the soil which leads to poorly defined crack edges at the surface. Finding the true depth of cracks can be difficult as well; flexible metal straps may be used to reach the bottom of torturous cracks. A geometry factor is often multiplied by the crack volume calculated from depth, width, and height to help account for the cross sectional area of the crack (Dasog and Shashidhara, 1993; Yassoglou et al., 1994).

Soil subsidence has been measured by installing anchors at various soil depths and measuring their movement relative to a fixed monument. These anchors are connected to a rod that extends to the soil surface for measurement and are covered with a sleeve to reduce interference from surrounding soil. The amount that each anchor moves vertically relative to the monument is translated into soil shrinkage or swelling, and by assuming that shrinkage is equidimensional (the same in all directions), vertical shrinkage can be used to predict horizontal shrinkage of the soil, indicating the volume of cracks that could occur in response to that shrinkage. More recently, the anchor method of measuring soil subsidence for use in crack volume prediction has been improved upon by insertion of magnets into the soil from a vertical bore-hole (Neely et al., 2014). These magnets move as the soil shrinks and swells and monitoring their location changes (using a position sensor) gives the change in soil layer thickness. Each soil layer is bounded by a magnet on the top and bottom of the layer. Measured changes in layer height may be translated to changes in volume assuming equidimensional shrinkage. The magnets may all be placed at the same x-y coordinate on the landscape, only changing their z coordinate as they are placed at different depths; whereas, the

anchors previously mentioned could not be placed on top of one another because the soil above the layer to be measured had to be removed. For this reason, the magnet system reduces uncertainty due to spatial variability across the landscape. Another improvement of this magnet system over the older anchor method is that the vertical bore-hole that is used to insert the magnets into the soil profile may be used as an access tube for a neutron moisture meter so that VWC measurements may be taken which include the volume of soil that the subsidence measurements are taken in.

The third in-field method of measuring soil crack volume is infilling. This method is time consuming and can only be done for a fixed water content since, unlike the physical measurements or the subsidence measurements, the infilling will not allow the soil to continue shrinking and swelling after measurement. However, the infilling method is more accurate than either of the above methods because it does not require an assumption of equidimensional shrinkage or estimation of geometry factors. The volume of cracks may be determined by taking photographs of the soil surface to capture the areal density of cracks and then excavating layers of soil and photographing the surface at each layer. By calculating areal density of the cracks for each layer and multiplying by the depth of the layer, crack volume for the whole profile may be found. Excavation requires complete destruction of the site. Of the three methods for on-site crack measurements, infilling of cracks provides the most accurate and high resolution option for finding crack volume on a small site. While the volume of cracks in the field is difficult to measure and is dynamic, these field measurements will be useful tools in comparing preferential flow paths that are modeled to cracked Texas clay soils.

Strategies for Modeling Water Flow in and Through Cracked Soils

Representation of water flow into and through soil is a key component of models used for agricultural decision making. Traditionally, soil water models and modules use Richards' equation (Richards', 1931) to represent this water flow through soils. Examples include 2DSOIL, which uses only Richards' equation and both the SPAW model and its derivative MUTillS (Porter and McMahon, 1990). A foundational assumption of Richards' equation is that the soil being evaluated has a continuous, homogenous matrix of solid particles, and this assumption is not valid for shrink-swell soils (Jury et al., 1991). When preferential flow paths (mesopores or cracks) are present in the soil, attempts have been made to "average over" the preferential flow paths by quantifying the total porosity of the system. This is done by measuring the hydraulic conductivity of the soil matrix and preferential flow paths together and representing them as one domain. As a result, soil hydraulic conductivity for Richards' solution is increased, so that water will travel deeper more quickly. This "fix" for preferential flow in a soil system fails to characterize the flow patterns associated with preferential flow and results, not in bypassing flow around soil peds, but in a continuous wetting front that travels deeper than the soil matrix hydraulic conductivity would have allowed. This approach does not represent the physics behind water flow through a cracking soil because it does not capture the by-pass flow behavior desired (Šimůnek et al., 2003). In addition to the lack of bypass flow that Richards' equation characterizes, its reliance on hydraulic conductivity makes it a poor choice to represent desiccation cracks, because the hydraulic conductivity of the system would have to be known for situations when the

cracks are closed, when the cracks are open, and likely for a range of crack volumes in between these two points (Bouma & Dekker 1978; Novák et al, 2000). This would require the addition of a new function to change the hydraulic conductivity with changes in crack volume (driven by changes in water content). This would demand an impractical number of measurements to characterize the system.

Rather than averaging the hydraulic properties of the whole soil, in this case the soil matrix and preferential flow paths, both areas may be characterized separately. The concept of representing two adjacent flow paths with different methods is referred to as a two-domain or dual-domain concept and it has existed since at least 1946 (Beven & Germann, 1982). The two-domain concept has been repeatedly used to model preferential flow in soils (Connolly, 1998; Šimůnek et al., 2003; Lepore et al., 2009). Almost without exception, Richards' equation governs flow in the matrix (also called the diffuse domain). Two-domain models differ in how they represent flow in the preferential domain (also called the macropore domain, the mesopore domain, or the source-responsive region).

The usefulness of models that consider preferential flow is becoming increasingly recognized. An example of a widely used model for agricultural and environmental decision making is the second version of the Root Zone Water Quality Model (RZWQM2) which is distributed by the United States Department of Agriculture's Agricultural Research Station in Fort Collins, CO. The RZWQM2 represents preferential flow in soils based on gravity flow by using Poiseuille's law (Ma et al., 2012). This two-domain representation of water flow is promising for capture of

the bypass flow behavior of cracking soils, however the dynamic nature of the preferential flow in soil cracks is not characterized. For example, the RZWQM2 model simulates preferential flow in root channels and worm tunnels which are considered to have a constant volume, whereas soil cracks and interpedal mesopores change volume over time with changes in water content.

Some attempts have been made to characterize shrink-swell behavior including the SWAP family of models, i.e. LEACHM, which represents preferential flow in desiccation cracks using a shrinkage characteristic and water loss (Kroes et al., 2000). This dynamic shrinkage transported water to depth more quickly, but neglected infiltration of water into the preferential flow path sides. Such infiltration is significant in cracked clay soils (Topp and Davis, 1981; Greve et al., 2010). Later modifications of SWAP included preferential flow paths that terminated at a variety of depths to better represent interaction with the soil matrix, but neglected shrink-swell properties of soils. Many models have been developed for preferential flow that could apply to desiccation cracks at a specific time, but do not account for the shrinking and swelling of cracks (Beven & Clarke, 1986; Porter & McMahon, 1990; Ahuja et al. 1993; Novák et al, 2000). To best represent infiltration for cracking, soils modules should include a preferential flow domain that can change volume with changes in water content and allow for redistribution of water at the interface of the preferential flow and soil matrix domains.

Alongside the issues of modeling flow in both soil cracks and the soil matrix, and of representing crack volume dynamically, is the issue of how to obtain the hydraulic

parameters that will be used in the preferential flow region. A common issue is the use of parameters that have only vague physical descriptions (Larsson & Jarvis, 1999). Even when parameters are better defined they are often extremely difficult to measure or accurately predict because of their variation across the landscape (Chen et al., 1993; Connolly, 1998; Šimůnek et al, 2003; Lepore et al., 2009; Nimmo, 2010). A review and comparison of preferential flow models found that two-domain models commonly require between 10 and 16 parameters (Šimůnek et al., 2003). The difficulties in using existing models such as Jarvis' MACRO, which simulates flow in macropores, are largely difficulties in obtaining parameters (Lepore et al., 2009). A more simplistic, closed form module was later introduced by Jarvis (2008), but he still noted that "very few published studies present data that are sufficiently detailed to properly test the suitability of the model."

An additional challenge is that these hydraulic parameters represent soil properties that are naturally variant across a landscape. Therefore, obtaining a number of parameters means, in actuality, mapping that number of parameters across the landscape of interest. Rather than map these properties, some prefer to obtain parameters by back calculation. This method uses measurements of the data that will later be model output (volumetric water content is an example) instead of measurements of the hydraulic parameters themselves (such as hydraulic conductivity). This model output is used to find (fit) combinations of parameters which could have produced the output. These fit parameters are then used for forward prediction. The great difficulty here is that the combinations of parameters that are fit in this manner are only correct for the fields in

which measurements were taken. Additionally, solutions are not unique, so several combinations of parameters may fit the same data. Using this approach, it is not known what the true hydraulic parameters of the site are, only a possible combination which could have led to the output gathered. This gives rise to many of the previously mentioned parameters that have no, or only vague, physical descriptions because they were developed by fitting data and not from hypotheses about the underlying physical mechanisms. Without a working hypothesis, it is difficult to modify the parameters as factors change across a landscape, and so measurement of the entire landscape to be modeled is necessary to continue parameter fitting. The need for a model that represents preferential flow paths with a dynamic volume that can be applied at a landscape scale without extensive measurements or parameter fitting has led to the evaluation of a current biophysical model that contains a dynamic preferential flow domain.

The Precision Agriculture Landscape Modeling System (PALMS) was developed at the University of Wisconsin, Madison to model biophysical processes associated with agricultural decision making. PALMS uses a 3-dimensional grid that interacts with topography and all major water transport phenomenon (rainfall interception, surface detention, runoff, runon, infiltration, soil water content, plant uptake of water, and drainage). Originally, PALMS used Richards' equation and one domain flow to simulate water flow through soil. A preferential flow component, the M&M module, which is based on soil structure, was incorporated into PALMS after its creation (Morgan, 2003; Lepore et al., 2009). The impact that soil structure has on soil hydrology is being increasingly recognized (Bouma & Dekker, 1978; Wu, et al., 1990; Chen et al., 1993;

Connolly, 1998). Currently, PALMS may be used either with a one domain module using Richards' equation or with a two-domain module using the M&M module. PALMS is an attractive option for the modeling of desiccation cracks because it already has the capability to model other agricultural processes of interest (tillage, addition of fertilizer, response of crops to weather changes, etc.) at a landscape scale. Of particular interest for modeling cracking soils, was the inclusion of COLE values that bound the shrinkage of soil peds based on water content. This description of shrinkage by COLE could potentially allow the shrinking and swelling of soil cracks to be modeled. This COLE value is available through the NRCS as an element of soil characterization data. For areas where COLE might not be adequately mapped, it may be estimated with a pedotransfer function based on available information such as clay content and mineralogy (McBratney et al., 2002). In fact, the NRCS offers estimates of COLE based on clay content that are easily available online (National Resource Conservation Service, 2014). COLE values (m m^{-1}) represent physical shrinkage measurements given by the following equation,

$$\mathrm{COLE} = \frac{{V_m}^{1/3} - {V_d}^{1/3}}{{V_d}^{1/3}}. \qquad [1.1]$$

where *Vm* is the total volume of the soil at field capacity, or -33 kPa, and Vd is the volume of the soil when oven dried to 105^{o}C, and is expressed one-dimensionally.

In the PALMS M&M module, preferential flow paths called mesopores are defined as cleavage planes that are created by the sides of adjoining soil peds, or structural units. Peds are represented as cubes in the M&M module (Fig. 1.3).

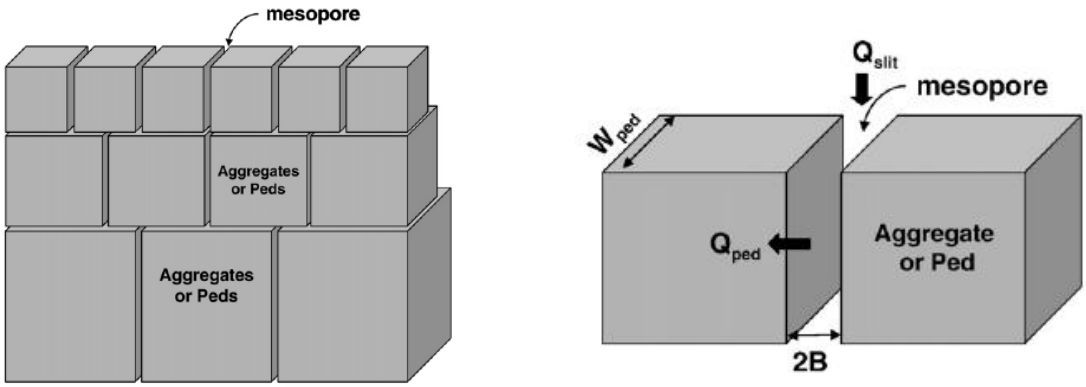

Figure 1.3. Ped geometry and mesopore structure. Adapted from Lepore et al., 2009.

The geometry and volume of cleavage planes available to conduct water is defined by the size of the soil peds. Ped size (width) is defined by 1) the ped's depth in the soil profile, 2) water content (θ), and 3) the COLE as follows:

$$\mathrm{w_{ped}}(\theta, \mathrm{z}) = \mathrm{w_{ped}}(\theta_{\mathrm{fc}}, \mathrm{z}) \left(1 - \mathrm{COLE} \frac{(\theta_{\mathrm{fc}} - \theta)}{(\theta_{\mathrm{fc}} - \theta_{\mathrm{ad}})}\right) \qquad [1.2]$$

where w_{ped} is the ped width at water content θ and depth *z*. The VWC at field capactiy is θ_{fc} and θ_{ad} is the VWC at air dry. The maximum ped width ($w_{ped,\theta fc}$) occurs at θ_{fc} because the ped is fully swollen. The $w_{ped,\theta fc}$ is multiplied by the term $\left(1 - COLE \frac{(\theta_{fc} - \theta)}{(\theta_{fc} - \theta_{ad})}\right)$, which accounts for the fraction of the maximum ped width that the ped will occupy at the new water content, θ. Multiplication by *COLE* in the previous term translates the water loss into ped width loss. The COLE value is in essence a fraction representing the volume of soil shrinkage that will accompany a volume of water loss. For example, if a ped has a COLE value of 0.1 and it loses 10 cm of water, it

would lose 1 cm of ped width and ped height (0.1 x 10 cm =1cm). Subtracting the soil width loss from the maximum width results in the ped width at the water content θ. Note that shrinkage in PALMS is considered to take place between field capacity and air dry. When the soil is at field capacity $(\theta_{fc} - \theta)$ is zero and the resulting ped width will be its maximun. When θ is at air dry (θ_{ad}) the full *COLE* value is subtracted from *1*, and the ped width will be at its minimum. The fully swollen ped size changes as a function of depth, becoming larger with greater depth in the soil profile because soils in the field generally have increasing ped size with depth. Because the distribution of ped size with depth changes from one soil to another, the ped size function may be altered to better reflect the ped sizes given in NRCS soil descriptions.

The loss of soil ped width described above generates an interaggregate slit, called a mesopore, between adjacent peds ($2B_{ped}$ in Fig. 1.3). B_{ped}, which is the half mesopore width, is calculated as follows,

$$B_{ped}(\theta) = B_{ped}(\theta_{fc}) + \left(\frac{w_{ped}(\theta_{fc},z) - w_{ped}(\theta,z)}{2}\right). \qquad [1.3]$$

The mesopore width for one side of one ped reaches its minimum, $B_{ped}(\theta_{fc})$, at field capacity and its maximum at air dry. The full mesopore width, which is $2B_{ped}$, is then available as a prefential flow path.

When no water is being applied to the soil surface, Richards' equation calculates water movement and storage in PALMS on a 15 minute timestep, including uptake of water by plant roots. When water is applied to the soil surface, it infiltrates via

unsaturated laminar flow through the six faces of the top layer of cubic peds and through the slits between peds. The Hagen-Poiseuille law, modified for flow through a planar slit (Bird et al., 1960), is used to characterize water flow through the mesopores as follows,

$$Q_{mp} = \frac{8{B_{ped}}^3 w_{ped} \rho g}{9\mu\left(w_{ped}+2B_{ped}\right)^2}. \quad [1.4]$$

Where B_{ped} half of the mesopore slit width, w_{ped} is the width of the mesopore, ρ is the density of water, μ is the viscosity of water, and g is acceleration due to gravity. The flux density of water moving through the mesopore is represented as Q_{slit} (Fig. 1.3). Darcy's Law is used to wet the peds from all six faces, accounting for ped geometry. Water is able to flow through the mesopores between peds and infiltrate into peds on a ten second time step. At the same time step as interpedal infiltration, this water flowing between ped interfaces can flow into the ped matrix by Darcian flow. This redistribution of mesopore water into the soil matrix is governed by the matirx potential of the soil ped and surface area of the ped. The amount of water entering the peds then increases ped water content (decreases ped matric potential) and decreases the speed of wetting. After 15 minutes of mesopore infiltration and redistribution the amount of water that flowed into the peds is applied as a positive source to the Richards' solution outside of the M&M module. Thus the PALMS preferential flow model essentially uses infiltration to facilitate rapid water movement in soils. More detailed discussions of the PALMS M&M module may be found in Lepore et al. (2009) and Morgan (2003). Because water does not have to fully saturate one layer of peds before the next layer can start wetting, by-pass flow is simulated in PALMS. The area available to transport water through

preferential flow paths is limited by the mesopore widths, which allows the shrink-swell potential (COLE) and the current water content to impact the volume of the preferential flow paths. In high shrink swell soils, COLE can increase $2B_{ped}$ volume during drying, allowing for more water flow. Therefore, PALMS already possesses the mechanism to generate preferential flow path volume of a drying shrink-swell soil. The appropriateness of using these preferential flow paths as a proxy for soil cracks needs to be evaluated for a shrink-swell soil.

Study Scope

The PALMS M&M module has the potential to address all three challenges in modeling water flow through soil cracks. The M&M model simulates water in two domains to address the challenge of preferential flow. The difficulty in obtaining parameters is addressed in the M&M model using soil morphological descriptions available through the NRCS. The dynamic nature of soil cracks is addressed using COLE to change the volume that is available for preferential flow. The PALMS M&M module has not been tested on cracking soils. The overall goal of this project is to seek answers to the following specific research questions regarding how well the PALMS M&M module represents a cracked soil system:

1. *How does the area of mesopores generated by the PALMS M&M module compare to field measurements of crack area?* Three soils with variable COLE values had crack volume measured at a specified water content. The area of cracks at several depths in the three soils will be compared with estimations of

soil mesopore area by PALMS using the COLE values and water contents measured when field crack volume measurements were taken.

2. *What is the influence of COLE values typical for shrink-swell clays on estimates of preferential flow path volume in the PALMS M&M module?* Because the M&M module includes COLE, allowing the soil mesopore size to change, it is desirable to determine the contribution of COLE during an infiltration simulation. Additional estimates of mesopore area will be plotted with varying COLE and soil moistures to better understand how strongly COLE influences preferential flow path volume in the M&M module and what influence these volume changes have on infiltration and redistribution of water.
3. *How well does the PALMS M&M module represent water flow on a cracked soil under intense rainfall?* Changes in the redistribution of water in a cracked soil profile will be assessed when A) PALMS with only Richards' equation is used and B) when the PALMS two-domain M&M model is used. Irrigation events when cracks are open will allow for the measurement of water redistribution with the neutron moisture meter (NMM). The quality of measurements for these redistribution curves will be considered in light of the known error associated with the NMM when water-filled cracks are present in the soil around the NMM access tube. Simulations of VWC generated using PALMS with Richards' equation will be compared to simulations of VWC generated using PALMS with the M&M module and also to the NMM measurements of VWC.

Answers to these three research questions will provide a better understanding of whether the PALMS M&M module, in its current state, can simulate water flow through a soil with open desiccation cracks so that PALMS may be used for agricultural decision making when soil desiccation cracks are present in the landscape.

CHAPTER II

PREFERENTIAL FLOW PATH MODELING

Introduction

Preferential flow paths in cracked soil change the physical process by which water infiltrates and redistributes in the soil. Generally, water passes through soil via air-filled paths and into soil peds. In shrink-swell soils, water may flow through the large mesopores, e.g. widths of 0.03 to 5 mm (Luxmoore et al., 1990), between soil peds or structural units and also through larger desiccation cracks, documented with widths up to 40 mm (Kishné et al., 2009). Separating the effect of these two types of preferential flow paths for modeling of water infiltration and redistribution for pedons and landscapes with the chosen model, the Precision Agriculture Landscape Modeling System (PALMS), is challenging. Moreover, it is not clear whether the distinction between cracks and mesopores is necessary in modeling infiltration or redistribution in cracked soil. The Mesopore and Matrix (M&M) module in PALMS does not recreate a geometry or distribution that matches observations of large desiccation cracks -it is not a model that simulates the large desiccation cracks observed in Texas Vertisols (Kishné et al.,2010). Rather, the M&M module represents interpedal preferential flow paths (mesopores) that temporally change in size according to the shrink-swell potential, or coefficient of linear extensibility (COLE), and changes in soil water content (Morgan 2003; Lepore et al,. 2009).

In the M&M module, size and geometry of mesopores is defined by size of soil structural peds, the width of the slits, and the COLE. The M&M module assigns the

same minimum mesopores width to all mesopores in a given soil horizon. Minimum mesopore width is assigned using the saturated hydraulic conductivity of a soil horizon, based on texture, in Rawls et al. (1992) look up table on soil hydraulic properties. Mesopore width can then become larger as peds shrink from water loss. Higher COLE values translate to more shrinkage, and therefore wider mesopore slits, at any given water content. Higher COLE values, which create wider slits, allow for greater infiltration at the soil surface and for greater volume of mesopores which allow water transport down the soil profile. This is the mechanism by which the COLE value impacts infiltration and vertical redistribution-by creating more mesopore volume that is available for preferential flow via Poiseuille's law in the M&M module. Horizontal mesopores are active in allowing water to infiltrate from the ped faces into peds via Darcy's law, but are not active for moving water down the soil profile.

Surface area of the peds drives horizontal redistribution by allowing water to move from mesopore space into the soil. The surface area for horizontal infiltration of mesopore water into the peds can be dramatically changed by changes in ped width. The M&M module is designed to represent descriptions of soil structure which are provided by the NRCS soil survey. Generally, smaller peds occur at the soil surface transitioning to larger peds at depth. All peds for a given depth layer are the same size. The M&M module has 23 layers extending to a depth of 2.5 m (more layers may be added to reach a depth of 5.5 m if data is available, but this is not required for simulations). The sigmoid equation which gives the ped width at each depth is,

$$w_{ped}(\theta, z) = w_{ped,0}(\theta) + \frac{(w_{ped,max}(\theta) - w_{ped,0}(\theta))}{1+10^{h log_{10}(\frac{c}{z})}}. \quad [2.1]$$

In equation 2.1, w_{ped} is the effective ped size as a function of depth (z) and water content (θ), $w_{ped,0}$ is the surface ped size, $w_{ped,max}$ is the largest ped size in the profile, h is the slope of the curve (dimensionless), and c is the depth at which the aggregate size is half way between the maximum and minimum aggregate sizes. Estimates for these values may be found using an official soil series description provided by the United States Department of Agriculture's National Resource Conservation Service (USDA NRCS). If h=1, the function takes an exponential shape and if h=2, the curve becomes sigmoidal. The desired shape will depend on the distribution of ped sizes with depth for the chosen soil series description.

To run the M&M module, nine parameters are required. Values are needed for $2B_{ped}(\theta_{fc})$, ψ_e, b, $K_{s,ped}$, $COLE$, $w_{ped,0}(\theta_{fc})$, $w_{ped,max}$, c, and h, where θ_{fc} is the volumetric water content (VWC) at field capacity. Each of these parameters has a default value in the M&M module for every soil texture so that the user need not measure them in the field. This project will focus on shrink-swell clay soils. The author does not suppose that the minimum slit width $(2B_{ped}(\theta_{fc}))$, air entry potential (ψ_e) of the soil matrix, or Campbell's pore size distribution index for the matrix (b), will be altered for the chosen soils. The saturated hydraulic conductivity of peds ($K_{s,ped}$) is set to one third of the Rawls et al. (1992) look-up table value for the soil textures following the recommendations of Lepore et al. (2009), which describes lower infiltration of water into peds because of clay film development (Gerke and Köhne, 2002). The COLE values are available from NRCS official soil series descriptions. The remaining four parameters are $w_{ped,0}(\theta_{fc})$, $w_{ped,max}$, c, and h, which are all parameters needed to calculate the width of a ped at a

given depth and water content ($w_{ped}(\theta,z)$, Eq. 2.1). These four parameters will be assumed from the official soil series description for the field location. Morgan (2003) and Lepore et al. (2009) discuss practical strategies for obtaining the parameters needed of the M&M module from established literature and routine measurements.

In chapter III the assumption that, when compared to PALMS with Richards', the gravity-driven flow which the M&M module uses for water flow through preferential flow paths will result in modeled infiltration and redistribution that is more similar to measurements in a Texas Vertisol with large surface cracks. The author's intention is to apply the M&M module in an attempt to capture the preferential flow behavior of cracking soils. In this chapter, to better understand how well the M&M model might represent preferential flow in a cracked Vertisol, the following questions are asked:

1. *How does the area of mesopores generated by the PALMS M&M module compare to field measurements of crack area?*
2. *What is the influence of COLE values typical for shrink-swell clays on estimates of preferential flow path volume in the PALMS M&M module?*

To address the first question, the total volume of mesopores that the M&M module generates was compared to crack areas previously found by infilling and excavation (Neely, 2014). To address the second question, changes in modeled infiltration and modeled soil VWC were compared across simulations with various COLE values.

Materials and Methods

Estimates of mesopore area with changing COLE

To answer question one, the mesopore area modeled using the M&M module was compared to field measurements of crack area as calculated from subsidence and from photographs of cement-filled cracks. Both the layer-subsidence method and the cement-filled cracks method of estimating crack volume were considered to be independent measures of estimating vertical, water-conducting, "cracking", pore space. The subsidence method assumes equidimensional shrinkage and that all shrinkage becomes crack volume. The cement method assumes all cracks conduct the poured cement. The subsidence based measurement the M&M module are expected to result in a greater crack area estimation than the cement method because they account for all preferential flow volume, not just large cracks. It is not know that the preferential flow behavior of a soil is governed only by cracks large which are visible, even though they are the most commonly measured.

A study by Neely (2014) measured subsidence and crack volume on Texas soils containing a COLE values ranging from 0.01 to 0.17 m m^{-1}. Four of the seven soils studied are considered (Table 2.1). All soils were found near College Station, TX (30°36′05″N, 96°18′52″W), and were under perennial grass and forb vegetation. Three of these sites (the three clays) showed visible cracks upon drying, and one site with a COLE value of 0.08 m m^{-1} had no visible surface cracks but is used for comparison (Table 2.1).

Table 2.1. USDA-NRCS classification of soils.

Soil Texture	COLE m m^{-1}	Soil Series	Taxonomic Class
Sandy clay loam	0.08	unidentified	
Clay	0.11	Burleson clay variant	fine, smectitic, thermic Udic Haplusterts
Clay	0.14	Ships clay	very-fine, mixed, active, thermic Chromic Hapluderts
Clay	0.17	Burleson clay	fine, smectitic, thermic Udic Haplusterts

Each soil was represented by a 3 by 3 m plot and all cracks within the plot were filled with a slurry of water and Type 1 white Portland cement (1:1 by volume). Plots were excavated in horizontal layers at approximately 5, 15, 30, 50, 70, and 90 cm. High-resolution digital photographs of each excavated surface were converted to binary images by Neely (2014) in order to estimate soil crack area for each layer (e.g. Figure 2.1).

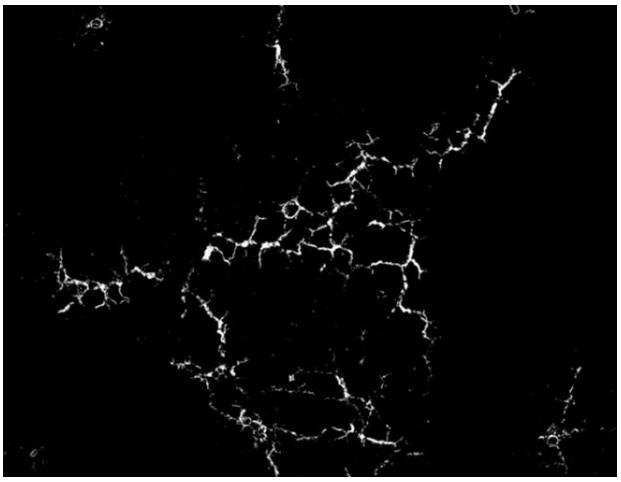

Figure 2.1. Binary image of excavated cement-filled cracks at 5 cm depth courtesy of Neely (2014).

Soil subsidence measurements were also collected for each soil layer that was photographed during the study. The magnet and sensor method was used to gather subsidence data (Neely et al., 2014). These measurements were used to calculate the areal volume of cracks (volume of cracks per unit area) based on vertical soil shrinkage using equation 2.2, a rearrangement of the Bronswijk (1989) equation by Neely (2014),

$$areal\ crack\ volume = \left(1 - \left(1 - \frac{L_1 - L_2}{L_1}\right)^{r_s}\right) * L_1. \quad [2.2]$$

In Eq. 2.2, L_1 is the initial soil layer thickness, L_2 is the final layer thickness, and r_s is a dimensionless factor, set at r_s=3 to represent equadimensional swelling. Areal crack volume, m^2 cracks m^{-3} of soil, was normalized by layer thickness, to m^2 cracks m^{-2} of soil. Then the depth-normalized values were multiplied by 0.64 to account for only vertical cracks that conduct water. For soil layers at 15, 30, 50, 70, and 90 cm, the area of mesopores produced by the M&M module, the area of cracks calculated in each photograph, and the area of cracks predicted by the Bronswijk equation were compared. The following is a discussion of how the area of mesopores per m^2 of soil is calculated for the M&M module. Figure 2.2 shows the geometry of peds and mesopores in the M&M module.

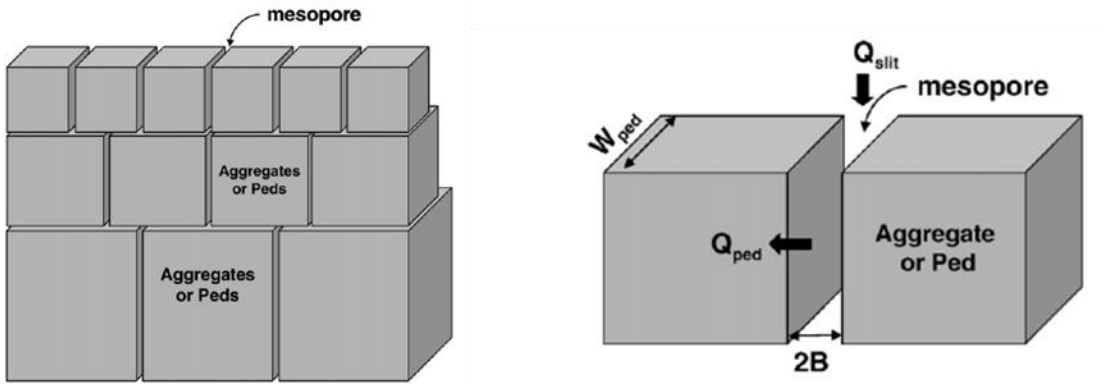

Figure 2.2. Ped geometry and mesopore structure. Adapted from Lepore et al., 2009.

Each ped is assigned one half of the six mesopores that surround it (*2B* in Fig. 2.2). Four of these half-mesopores are vertically oriented and are able to conduct water via laminar flow, using Poiseuille's law. Half-mesopore area is calculated as $w_{ped} * B_{ped}$. The total mesopore area for one ped is $2 * (w_{ped} * 2B_{ped})$. Dividing the area of mesopores assigned to a ped by the total area (area of ped plus area of mesopores) gives the m^2 of mesopores m^{-2} of total area as in,

$$\frac{2*(w_{ped}*2B_{ped})}{(w_{ped}+2B_{ped})^2}. \quad [2.3]$$

Equation 2.3 represents this mesopore area and the area increases with water loss because w_{ped} at a given depth shrinks with water loss based on the *COLE* value as in,

$$w_{ped}(\theta, z) = w_{ped}(\theta_{fc}, z)\left(1 - COLE\,\frac{(\theta_{fc}-\theta)}{(\theta_{fc}-\theta_{ad})}\right). \quad [2.4]$$

The study by Neely (2014) provides COLE values and water contents (θ) at the depth and time of crack filling and excavation for the four soils in Table 2.1. Default values

for water content at field capacity (θ_{fc}) and water content air dry (θ_{ad}) were taken from the M&M module's texture based tables originally found in Rawls et al. (1992). Values for $w_{ped}(\theta_{fc}, z)$ were calculated using Eq. 2.1. The width of the surface peds at field capacity ($w_{ped,0}(\theta_{fc})$) were found in the official soil series description. The Burleson clay, for example, had a medium subangular blocky structure for the surface horizon. This represents surface ped widths between 1 and 2 cm (National Soil Survey Center, 2002). Lepore et al. (2009) discussed that, because not all mesopores are likely to conduct water, the effective aggregate size might be larger than the mean structure class. Because the structure distinctness was reported as moderate, it is assumed that every other ped intersection would conduct water, therefore $w_{ped,0}(\theta_{fc})$=4 cm was used instead of 2 cm. The $w_{ped,max}$ in the Burleson profile is 20 cm as found in the soil series description.

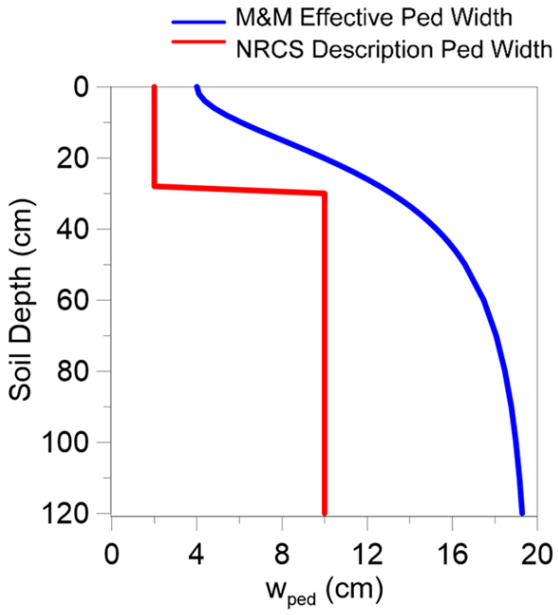

Figure 2.3. Ped width with depth for Burleson description and Burleson effective aggregate size used by the M&M module.

The remaining values needed to calculate the ped widths are *c*, which is the depth at which the ped size is the half way between its minimum and maximum, and *h* which is a dimensionless parameter that influences the shape of the curve. The *c* value was set to be 0.26 m, and *h*=2 was chosen for a sigmoidal curve shape. Figure 2.3 shows how estimated effective aggregate size for the Burleson clay relates to the NRCS description.

The mesopore half-width is a function of the half-width at field capacity, plus any gain in width due to ped shrinkage,

$$B_{ped}(\theta) = B_{ped}(\theta_{fc}) + \left(\frac{w_{ped}(\theta_{fc},z) - w_{ped}(\theta,z)}{2}\right). \qquad [2.5]$$

The value for $B_{ped}(\theta_{fc})$ may be found in the PALMS source code in a texture-based look-up table. For clay, the minimum slit width is 0.0062 cm (B_{ped}=0.0031 cm) and for the sandy clay loam soil the minimum slit width is 0.0098 cm (B_{ped} =0.0049 cm). Equations. 2.4 and 2.5 are used to calculate mesopore area per soil area at a given water content in equation 2.3. For comparison with other cracking estimates, the mesopore area in Equation 2.3 at field capacity (the minimum mesopore area) was subtracted from Eq. 2.3 at the field measured water content.

These M&M equations yield the area of vertically oriented mesopores generated at the same soil depth, water content, and COLE value that was measured when the photographs of cement-filled cracks were taken in the field. The comparisons of crack area estimates between the M&M module, Bronswijk equation predictions from subsidence measurements, and photographs of cracked soil were made to evaluate how the estimates of hydraulically-active preferential flow paths in the M&M module relate to the large cracks found in Texas Vertisols.

PALMS Simulations

Twenty PALMS simulations were run with variable COLE values to better understand how COLE affects infiltration and redistribution in PALMS. Four precipitation scenarios, which matched irrigation events used in chapter III, were used for PALMS input (Table 2.2). Two events simulated a one-hour rainfall of 22 mm and two events simulated longer storms in which 66 mm of rainfall fell. The third irrigation event was the only one in which ponding was observed in the field.

Table 2.2 Irrigation Events.

Irrigation Event	Plot	Date	Duration	Intensity	Water Applied
			hr	mm hr^{-1}	mm
1	2	7/30/2013	1.25	22	22
2	1	8/02/2013	8	17	66
3	2	8/13/2013	24	14	67
4	1	9/27/2013	1.25	22	22

For each irrigation event, five PALMS simulations were run. One of these five simulations used one-domain water flow (Richards' equation). The other four simulations for each event used the M&M module. COLE values for these four M&M

simulations were 0.01, 0.05, 0.10, and 0.17 m^3 m^{-3}. The average VWC for the five NMM access tubes in each plot was used as the initial soil VWC at the start of each PALMS simulation. The parameters for these five simulations were the default parameters in PALMS. The saturated hydraulic conductivity of the ped ($K_{s,ped}$) was taken from the Rawls et al. (1992) tables. The air entry potential (ψe) was 0.370, Campbell's exponent for the moisture release equation (b) was 7.6, and the slit width at field capacity ($2B_{ped}(\theta_{fc})$) was 0.006 cm. Using the Burleson soil series description, h was 2, c was 26 cm, $wp_{ed,0}(\theta_{fc})$ was 4 cm, and $w_{ped,x}(\theta_{fc})$ was 20 cm. Relevant output for these simulations includes the $w_{ped}(\theta,z)$, $2B_{ped}(\theta,z)$, θ, and infiltration.

Results and Discussion

M&M Module Preferential Flow Paths Compared to Cracks in the Field

Table 2.3 gives the fraction of the plot area that was occupied by cracks in m^2 m^{-2} for each soil layer that was excavated and photographed. Also shown is the fraction of plot area that the M&M module assigns as mesopores, for the depth, water content, soil type, and COLE value that was measured in the plot at the time of excavation. Crack area based on subsidence measurement using the Bronswijk approach (Eq. 2.3) is also shown.

The area of cement-filled cracks equaled as much as 29% and as little as 0% of the area predicted to be mesopores by the M&M module. The cement-measured crack areas were smaller than both the M&M module estimates and the Bronswijk predictions for all soils and depths, with the exception of the top layer of the Ships clay, which

showed no subsidence. Bronswijk area estimates were smaller than M&M area predictions, except in the sandy clay loam soil.

The difference between the PALMS M&M module and the Bronswijk model may be explained by the different mechanisms by which the models calculate the preferential flow area. The M&M module was using COLE and water content while the Bronswijk model uses subsidence. If any of the vertical shrinkage does not result in soil layer subsidence, then the Bronswijk model will not capture that vertical shrinkage and so will not generate horizontal shrinkage that will contribute to the crack area which is being assessed.

It is likely that shrinkage which occurs in well-structured soils, like the clays the Study conducted by Neely (2014), might take the form of interpedal voids (mesopores) that would not contribute to subsidence in the way that large cracks would. The M&M module makes no distinction between shrinkage that will result in subsidence and shrinkage that will not.

Table 2.3. Comparing fraction of area occupied by cracks as measured in the field to mesopore estimates using the M&M module, the Bronswijk equation, and cement-filled crack data. The latter two courtesy of Neely, 2014.

				--------Simulated Crack Area--------			Percent of M&M Area	
Soil	Depth cm	COLE m m^{-1}	θ m^3 m^{-3}	Cement m^2 m^{-2}	Bronswijk m^2 m^{-2}	M&M m^2 m^{-2}	Cement %	Bronswijk %
Sandy Clay Loam	5	0.07	0.20	0.000	0.072	0.107	0	67
	15	0.07	0.21	0.000	0.116	0.093	0	124
	30	0.02	0.25	0.000	0.054	0.010	0	529
	50	0.02	0.25	0.000	0.031	0.009	0	325
	70	0.04	0.22	0.000	0.011	0.051	0	22
	90	0.04	0.16	0.000	0.011	0.105	0	11
Burleson Clay Variant	5	0.12	0.14	0.015	0.206	0.338	4	61
	15	0.11	0.19	0.014	0.073	0.278	5	26
	30	0.10	0.25	0.006	0.035	0.205	3	17
	50	0.11	0.30	0.002	0.040	0.164	1	25
	70	0.12	0.33	0.002	0.025	0.130	1	20
	90	0.11	0.36	0.001	0.030	0.080	1	38
Ships Clay	5	0.14	0.27	0.011	0.000	0.250	4	0
	15	0.15	0.26	0.019	0.159	0.261	7	61
	30	0.14	0.30	0.011	0.058	0.194	6	30
	50	0.14	0.34	0.009	0.088	0.149	6	59
	70	0.15	0.34	0.006	0.114	0.151	4	75
	90	0.16	0.34	0.002	0.120	0.149	2	81
Burleson Clay	5	0.16	0.22	0.045	0.143	0.342	13	42
	15	0.16	0.21	0.039	0.126	0.363	11	35
	30	0.17	0.30	0.034	0.106	0.242	14	44
	50	0.17	0.34	0.030	0.084	0.177	17	47
	70	0.17	0.36	0.025	0.071	0.135	19	53
	90	0.17	0.38	0.026	0.045	0.089	29	51

Both of the models produced larger areas for preferential flow than the areas of large, cement-filled cracks. Of the cracking clays, the Burleson Clay mesopore areas were closest to the cement-filled crack area, with crack areas averaging 17% of the M&M mesopore area. The area of cement-filled cracks for the Ships clay averaged 5% of the M&M mesopore area, while the cement-filled cracks of the Burleson Variant averaged only 3% of the M&M mesopore area. The findings (larger values of predicted preferential flow area than the area that is measured) are not unprecedented. Another study of cracking soil, which included Burleson clay, found that using COLE to predict crack volume yielded volumes more than ten times greater than the crack volumes predicted using hand measurements (Rivera, 2011).

COLE and the Bronswijk equation account for all forms of soil shrinkage, not only shrinkage that takes the form of large, visible cracks. The M&M module agrees more closely with the Bronswijk equation than it does with the images of cement-filled cracks (Table 2.3). When considering all depths for all soils, the Bronswijk equation accounted for 45% of the M&M module's mesopore area. This excludes the 30 and 50 cm depths for the sandy clay loam, which did not shrink in the M&M module because the water contents were above field capacity for a sandy clay loam in PALMS. On average, the Bronswijk equation accounted for 45% of the preferential flow path area in the Burleson profile, 51% in the Ships profile, 31% in the Burleson variant, and 56% in the sandy clay loam. The two models agree in magnitude with one another better than either does with the cement-filled crack area because they both consider soil shrinkage that is not confined to large cracks that can be filled with cement. Though the M&M

module generated mesopore area for the sandy clay loam, no cracking was observed in the field. This indicates a threshold where COLE values do not result in soil cracking. The other three soils have cement-filled crack areas that are linearly related to M&M module mesopore estimates (Fig. 2.4). The M&M estimated mesopore area is more strongly linearly related to the cement-filled cracks than to the Bronswijk estimates for the Ships and Burleson variant and is comparable for the Burleson. The M&M module estimates are also more strongly linearly related to the cement-filled cracks than are the Bronswijk predictions. When the M&M module estimates are plotted against the cement-filled crack area, the slopes of the linear fit line for Burleson, Burleson variant, and Ships clay are 13.56, 15.64, and 7.67, respectively (Table 2.4). These slopes are close to the overestimation of cracking by ten times that Rivera (2011) found when using COLE to predict cracking.

The preferential flow behavior of a soil is not governed only by cracks which are visible. In fact, it was those preferential flow paths not visible to the human eye that prompted the creation of the M&M module and its addition to PALMS. The sandy clay loam in this study better represents the soils that the M&M module was first validated on than do the shrink-swell clays.

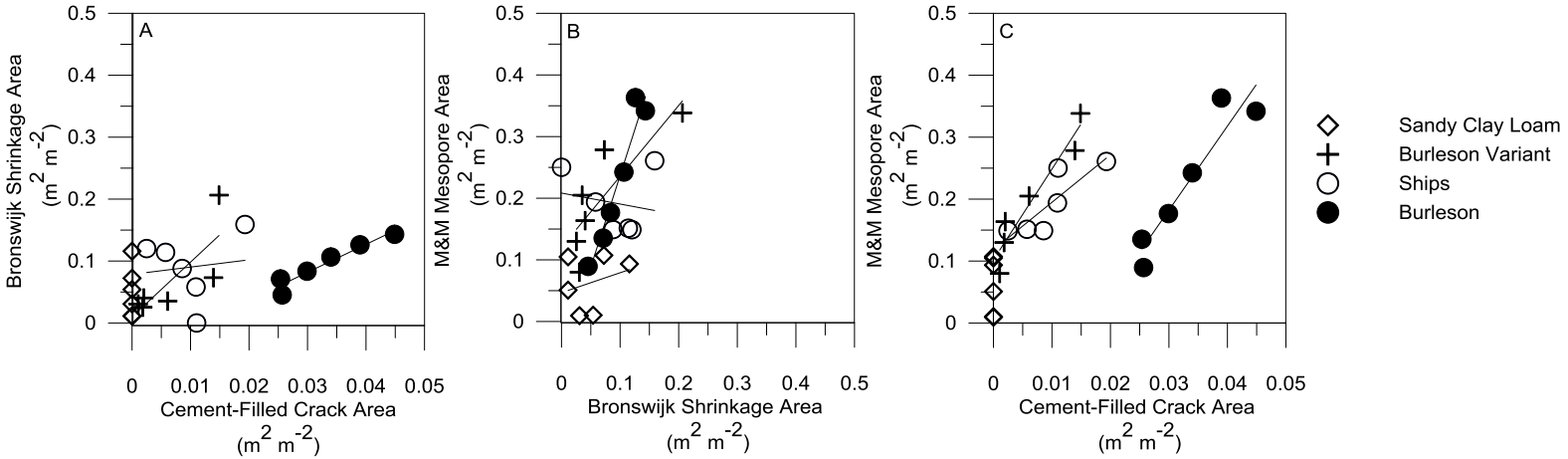

Figure 2.4. Scatter plots of predicted area of cracks/mesopores over ground area for A) Bronswijk equation and cement-filled cracks, B) M&M module and Bronswijk equation, and C) M&M module and cement-filled cracks

Table 2.4. Linear fits and Pearson correlation coefficients (r^2) values for Fig. 2.4.

	Burleson Clay		Burleson Variant		Ships Clay		Sandy Clay Loam	
	linear fit	r^2	linear fit	R^2	linear fit	r^2	linear fit	r^2
M&M vs. cement-filled cracks	13.56*x-0.22	0.89	14.64*x+0.10	0.92	7.67*x+0.21	0.78	0.0*x+0.06	1
M&M vs. Bronswijk	2.97 *x-0.06	0.94	1.15*x+0.12	0.70	-0.18*x+.21	0.04	0.32*x+0.05	0.08
Bronswijk vs. cement-filled cracks	4.52*x-0.05	0.93	8.82*x+0.01	0.63	1.17*x+.08	0.01	0.0*x+0.05	1

The sandy clay loam had no visible cracking, yet the M&M module generated preferential flow areas as large as 0.105 m^2 m^{-2} of mesopores. The addition of mesopores using the M&M module improved PALMS simulations on silt loam and silty clay loam loess soils in Wisconsin (Lepore et al., 2009). The fact that preferential flow in soils does not depend on visible cracks gives us confidence to apply the M&M module in an attempt to capture the preferential flow behavior of shrink-swell soils.

Sensitivity of M&M Module Preferential Flow Paths to COLE

Higher COLE values produce larger slit widths ($2B_{ped}$). A larger $2B_{ped}$ creates more capacity for water to infiltrate and to be moved down the soil profile. However, modeling results show that there is more capacity than water at even a high intensity rainfall event and for the lowest COLE value. In both moist and dry antecedent soil moisture, the COLE made no difference to infiltration and little difference to VWC when the M&M module was used. The soil profile wet and infiltrated differently for M&M module simulations as compared to simulations when the M&M module was off (Figs. 2.5 to 2.8). When irrigation begins, $2B_{ped}$ shrinks. Slits clearly shrink at 5 cm deep in all events. Slit width for all COLE values converge toward the minimum as the peds wet. $2B_{ped}$ at 5 cm depth for Event 1 does not reach the minimum except at the lowest COLE (Fig. 2.5). Event 1 had drier soil than Events 3 and 4 and had less water applied than Event 2. Events 2 and 3 reached the minimum $2B_{ped}$ at 5cm depth for every COLE (Fig. 2.6 and 2.7), while Event 4 reached the minimum $2B_{ped}$ at a 5 cm depth for all but the highest COLE (Fig. 2.8).

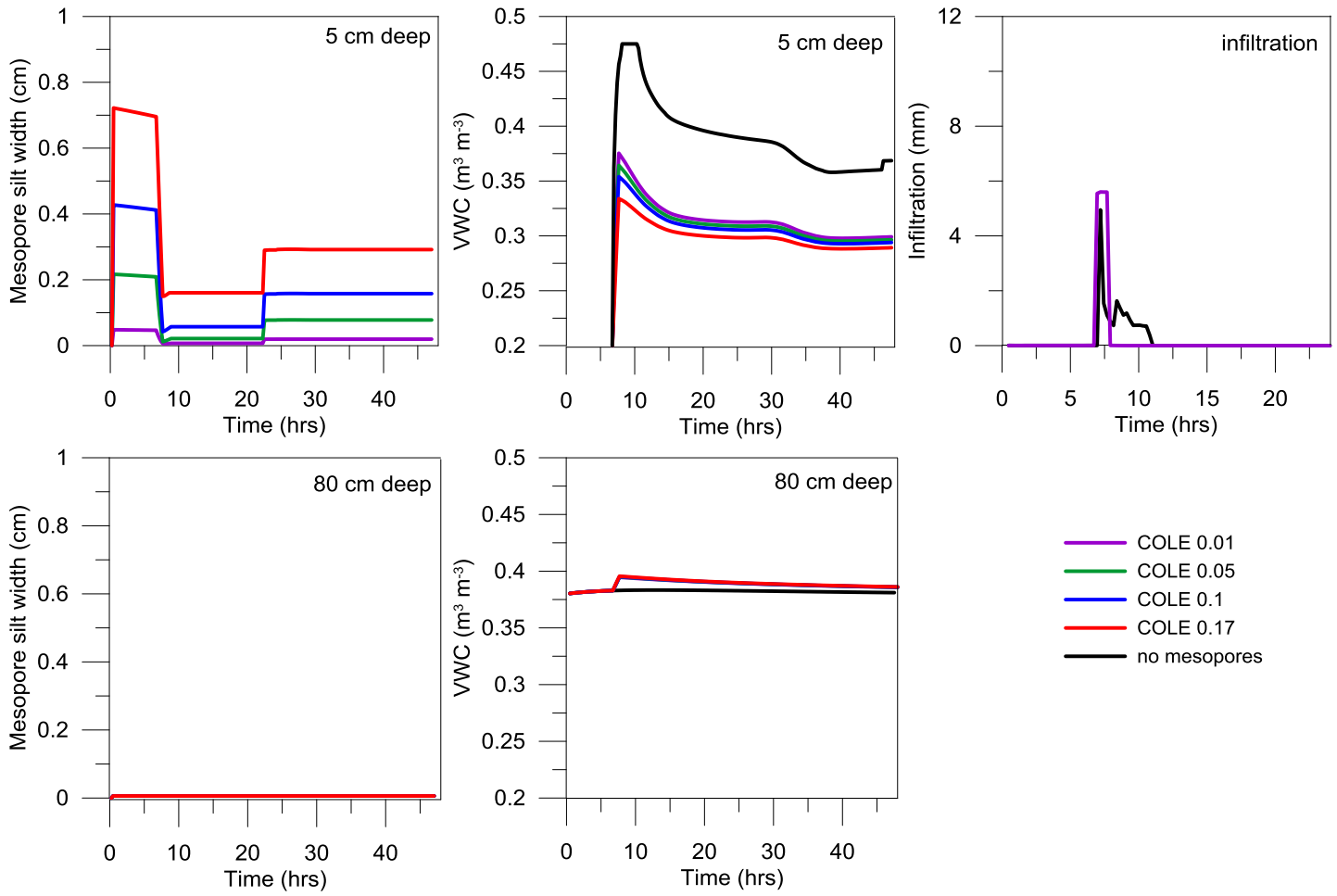

Figure 2.5. Event 1 (dry initial water content and 22 mm of water added) slit width at 5 and 80 cm depths, volumetric water content (VWC) at 5 and 80 cm depths, and surface infiltration are shown for 2.2 days for all PALMS simulations.

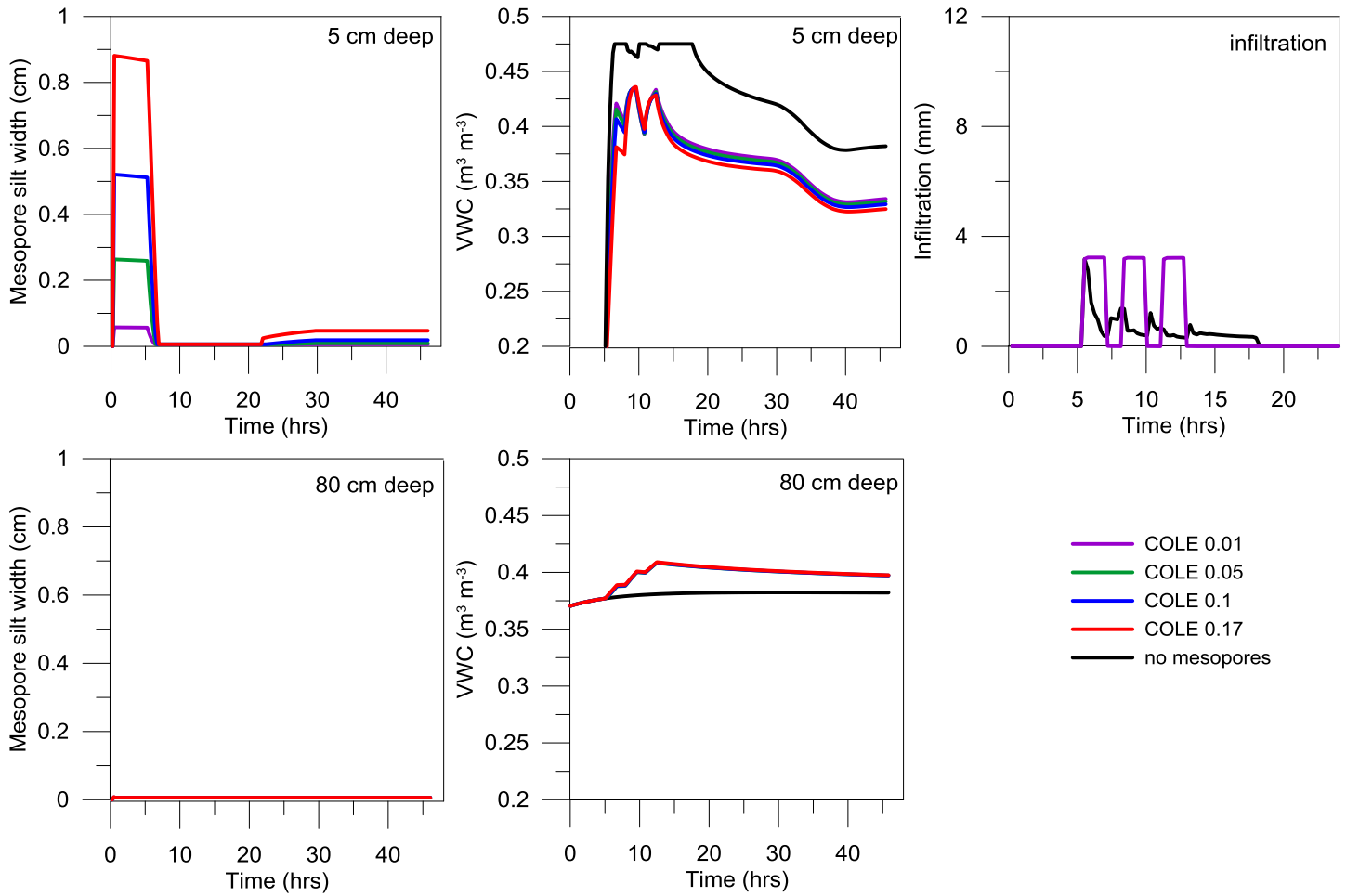

Figure 2.6. Event 2 (dry initial water content and 66 mm of water added) slit width at 5 and 80 cm depths, volumetric water content at 5 and 80 cm depths, and surface infiltration are shown for 2.2 days for all PALMS simulations

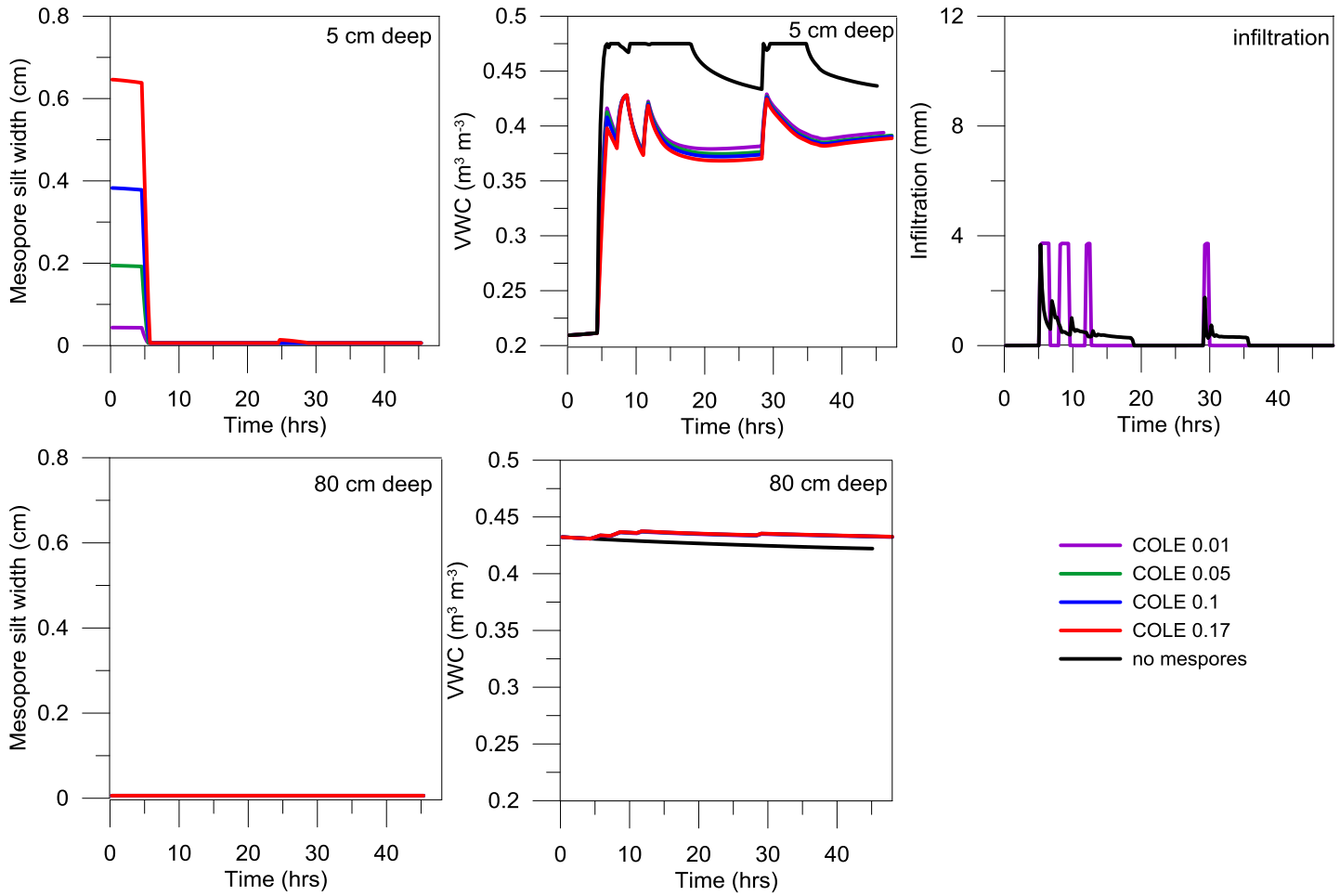

Figure 2.7. Event 3 (wet initial water content and 66 mm of water added) slit width at 5 and 80 cm depths, volumetric water content at 5 and 80 cm depths, and surface infiltration are shown for 2.2 days for all PALMS simulations.

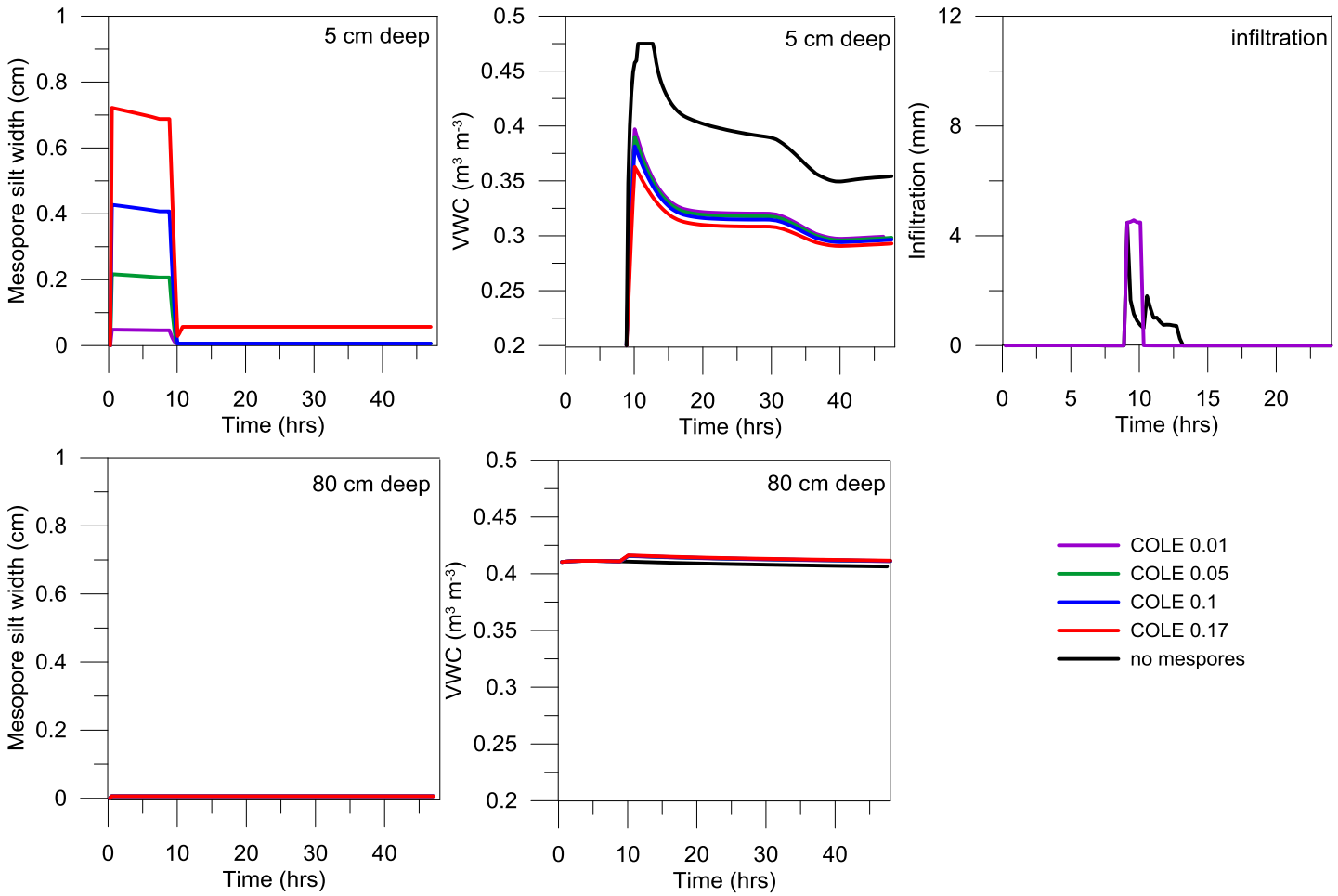

Figure 2.8. Event 4 (wet initial water content and 22 mm of water added) slit width at 5 and 80 cm depths, volumetric water content at 5 and 80 cm depths, and surface infiltration are shown for 2.2 days for all PALMS simulations.

At an 80 cm depth, $2B_{ped}$ shows very little response to irrigation in all events because $2B_{ped}$ was already near its minimum and VWC changes were small. The M&M module calculates water moving into a ped using the equation,

$$Q_{ped,s} = \frac{2k_{s,ped}\psi_e b}{g w_{ped(\theta,z)}}\left(1 - \frac{\theta}{\theta_s}\right). \quad [2.6]$$

Where $Q_{ped,s}$ ($m^3\ m^{-2}\ s^{-1}$) is the flux density of water moving into the ped and θ_s is the water content at saturation (0.475 $m^3\ m^{-3}$). Using $w_{ped(\theta,z)}$=0.185 m (the ped size at 80 cm), θ=0.36, and the PALMS M&M module parameter values chosen for the simulations, 9.42 x 10^{-5} $m^3\ m^{-2}\ s^{-1}$ of water entered the peds at 80 cm deep. The movement of water through the mesopores in the M&M module began when irrigation started and stopped when irrigation ended. The volume of the peds at 80cm depth is 0.006 m^3, and with a flux density of water at 9.42 x 10^{-5} $m^3\ m^{-2}\ s^{-1}$, over one hour of irrigation, the θ increased by 0.015 $m^3\ m^{-3}$. This small increase in θ is not easily seen in Figs. 2.5-2.8. For the short period of water residence in the macropores (one hour), the low hydraulic conductivity of the clay soil (1.7 x 10^{-7} m s^{-1}) results in small changes in VWC.

Higher COLE values do not change the infiltration rate of the water in any simulation using the M&M module (Figs. 2.5-2.8). The M&M module, even with a COLE value of 0.01, was able to allow all of the water in every irrigation event to infiltrate without ponding. The PALMS model without the M&M module, which uses Green and Ampt for infiltration, ponded water in all events. The author's field observations indicate ponding only occurred in Event 3. Modeled ponding and drainage are discussed in Chapter III.

The VWC is only slightly influenced by the COLE value for the M&M module simulations (Figs. 2.5 to 2.8). The greatest difference in volumetric water content across all COLE values and over all irrigation events was less than 0.05 m^3 m^{-3}. In each event, one 15 minute time step had a difference of about 0.04 m^3 m^{-3} between the highest and lowest COLE simulations. Volumetric water contents for the M&M module simulations converged with time.

Soil water content for the simulations which did not use the M&M module was very different from the M&M simulations. The water content at 5 cm deep saturated when the M&M module was not used, where as they did not saturate when the M&M module was used. As well, at 80 cm deep the soil did wet slightly in the M&M module simulations but did not when the M&M module was absent.

Summary

The M&M module generates more volume for preferential flow than observations of desiccation cracks which were filled with cement and photographed. However, the relationship between desiccation cracks and M&M estimates is highly linear. The linear relationship suggests that the M&M module is capturing the mechanism of the desiccation cracks but the understanding of crack volume is not correct. The M&M module's mesopore volume predictions align better with the Bronswijk predictions of soil shrinkage than with the crack volume measured. This outcome is expected because both M&M and the Bronswijk estimation are based on similar assumptions of crack-ped geometry.

The COLE value has a clear role in the mesopore width, and therefore the mesopore volume in PALMS. However, under the two high intensity infiltration events, the differing COLE values do not translate into noticeable changes in water infiltration or redistribution (volumetric water content profiles). The magnitude of changing a COLE value within the reasonable range of COLE values (0.01-0.17) has less impact than the presence/absence of the M&M module.

These findings led to testing the M&M module predictions against measurements of the redistribution of water in a cracked Texas Vertisol. The usefulness of this model may be assessed in how well it represents the behavior of water in the field. Further tests will compare the M&M to field observations of VWC with depth, runoff, and drainage.

CHAPTER III

MODELING WATER REDISTRIBUTION IN A CRACKED VERTISOL

Introduction

Water infiltration and redistribution in cracking clay soils are influenced by the presence of preferential flow paths in the soil (Topp and Davis, 1981; Novák et al., 2000). Measuring redistribution of water in cracking soils is difficult because of the changing volume of desiccation cracks and interpedal mesopores, but an understanding of redistribution will be useful in the development of models for landscape scale decision making on shrink-swell soils.

Studies of infiltration events have shown a significant influence of soil cracks and structure on infiltration and redistribution of water in soils. Topp and Davis (1981) used time-domain reflectometry (TDR) to measure water content changes during irrigation events on cracked clay soil. The TDR measurements showed that soil nearer to cracks tended to wet up more quickly, that water appeared to bypass portions of the soil matrix (wetting occurred at 10 to 30 cm depth but at neither the 0 to10 cm depth nor the 30 to 60 cm depth) and that crack flow did not begin until 2 hrs after the irrigation started. The findings of this study show non-uniform wetting both vertically and horizontally. Bouma and Dekker (1978) conducted infiltration events on four dry clay soils that included a dye tracer study for the purpose of determining the depth of infiltration via mesopores and cracks. The study found that soil structure strongly influenced the infiltration of water (stronger structure caused deeper infiltration), that

small areas of the ped faces (~2%) came in contact with the infiltrating water, and that by-pass flow occurred in the dry clay soils.

The need to characterize preferential flow paths for modeling of rainfall partitioning and redistribution has led to the development of models that incorporate soil structure and/or representations of preferential flow paths (Morgan, 2003; Šimůnek et al., 2003; Nimmo and Mitchell, 2013). The goal is to test one such model, the Precison Agriculture Landscape Modleing System's Mesopore and Matrix moduule (PALMS M&M module) by comparing PALMS M&M module simulations with measurements of redistribution of water in a cracked Texas Vertisol. Two sets of measurements were used for such comparisons, plot-scale irrigation events with hourly measurements of soil volumetric water content (VWC) and small watershed observations of soil VWC over a period of months with bimonthly soil moisture observations. The plot-scale irrigation events were conducted by the author and the watershed scale measurements were collected from a previous study (Dinka et al., 2012). Field measurements of volumetric water content under four infiltration events were collected using a neutron moisture meter (NMM) at the plot scale. The measurements were compared to the PALMS simulations with and without the M&M module turned on.

A second set of PALMS simulations were developed for a Houston Black clay landscape in Riesel, Texas. Topography and historical weather data from a 4.4 ha Vertisol watershed in Riesel, Texas were used to run PALMS simulations with and without the M&M module. NMM readings taken in 2008, 2009, and 2010 across the

landscape allowed us to evaluate which one of the two modeling approaches (M&M on or off) better represents measured soil moisture over a longer period of time.

Materials and Methods

Plot Experiment

Irrigations were done on two 10 by 10 m plots located at the Texas A&M University's Riverside Campus (30°38'03.1"N 96°28'58.1"W). Plots were separated from one another and surrounding soil by a hydraulic barrier that was created by digging a 60 cm trench extending to a depth of 120 cm, lining the inside of the trench with plastic, and repacking the soil. Soil on the plots was a Burleson Clay (fine, smectitic, thermic Udic Haplustert) that was uncultivated and under native grasses and forbes. Slope was less than 0.01 m m^{-1}. Each plot was used for two irrigation events; the first set of events had drier soil conditions previous to irrigation than the second. Each plot had one irrigation with 66 mm of water applied and one with 22 mm of water applied (Table 3.1).

Table 3.1. Irrigation events.

Irrigation Event	Plot	Date	Duration	Intensity	Water Applied
			hr	mm hr^{-1}	mm
1	2	7/30/2013	1.25	22	22
2	1	8/02/2013	8	17	66
3	2	8/13/2013	24	14	66
4	1	9/27/2013	1.25	22	22

Trailer mounted water tanks were used to transport water to the site. The water source was municipal tap water for the Riverside Campus of Texas A&M University. Honda multi-purpose WMP20x pumps were used to pump the water out of the tank and through three lines of ½ inch PVC pipe on to each plot. Nine Hunter® PRO-SPRAY sprinklers, outfitted with Rainbird® 18-VAN nozzles were attached to the PVC lines for uniform irrigation across each 10 by 10 m plot. Irrigations were not continuous because VWC measurements were taken during the irrigation events. Typically soil moisture measurements were taken after one tank of water was emptied. One tank held ~600 gallons-equivalent to 22 mm of water on the plots. For soil moisture measurements, plywood planks were placed on the soil surface to reduce disturbance from traffic and removed after measurement and before irrigations resumed. The irrigation intensities in Table 3.1 represent the amount of water applied divided by the time during which the sprinklers were actively applying water. The duration in Table 3.1 includes the whole period of the event, including times when the sprinklers were not running. In irrigation Event 3, water began to pond after ~56 of 66 mm of water had been applied. To avoid surface routing of water within the plot, irrigation was stopped and the plots tarpped to minimize evaporation. This took place 7.5 hours after the beginning of the irrigation event. The next day, 25 hours after the start of the irrigation event, the remaining 10 mm of water was applied to the plot.

Neutron Moisture Meter Measurements

Five aluminum NMM access tubes made of irrigation tube were installed to a depth of 1.3 m in each plot (Fig. 3.1). The outer diameter of each access tube was 5.05

cm (2 inches) The access tubes were identified by the plot number (1 or 2) and a tube number (1 to 5). A NMM was used to measure volumetric water content (VWC) at nine soil depths for each access tube. To install NMM access tubes, a 5.04 cm hole was hand-augured using a 5.04-cm o.d. bucket auger to a minimum depth of 140 cm and a thin-walled aluminum irrigation tube was inserted into the hole. NMM readings were taken at 10, 20, 30, 40, 50, 60, 80, 100, and 120 cm depths, and NMM count time was set to 32 seconds.

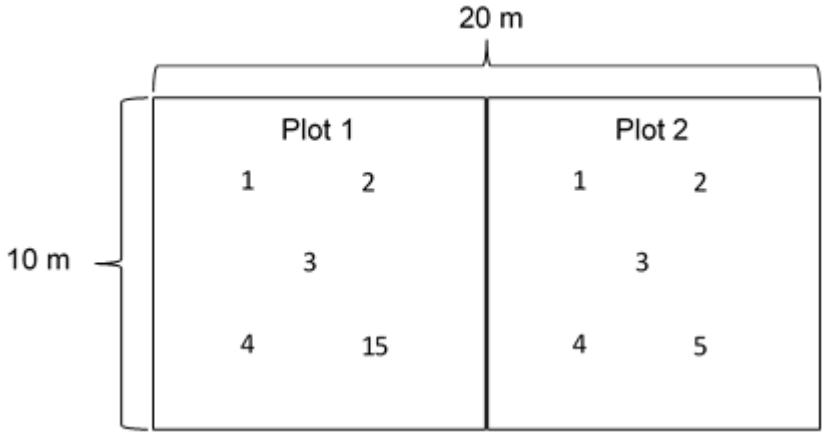

Figure 3.1. Layout of irrigated plots at Riverside campus including neutron moisture meter access tube placement.

The NMM (ICT International, 2013) was calibrated on-site. Four calibration locations surrounding the research plot were chosen for installation of NMM access tubes. At each location, a NMM access tube was installed and NMM readings were taken in 10 cm intervals to a depth of 150 cm. Then, soil cores were pulled to a depth of 170 cm using a hydraulic probe. Volumetric water content was measured for each core

in 10 cm sections, beginning with the 5 to 15 cm depth. The VWC from all cores that surrounded each access tube were averaged and plotted with the NMM count ratio for the location. Calibrations included soil at a dry soil moisture condition, which was cracked, and two calibrations after irrigation so that cracks were not found. The lowest volumetric water content in the calibrations was 0.277 m^3 m^{-3} and the highest was 0.429 m^3 m^{-3}. A calibration line was developed for 5 to 15 cm depth NMM readings (n=4, r^2 = 0.95, RMSE = 0.011 m^3 m^{-3}) and a separate calibration line was used for NMM readings from 15 to 160 cm (n=58, r^2 = 0.86, RMSE = 0.014 m^3 m^{-3})

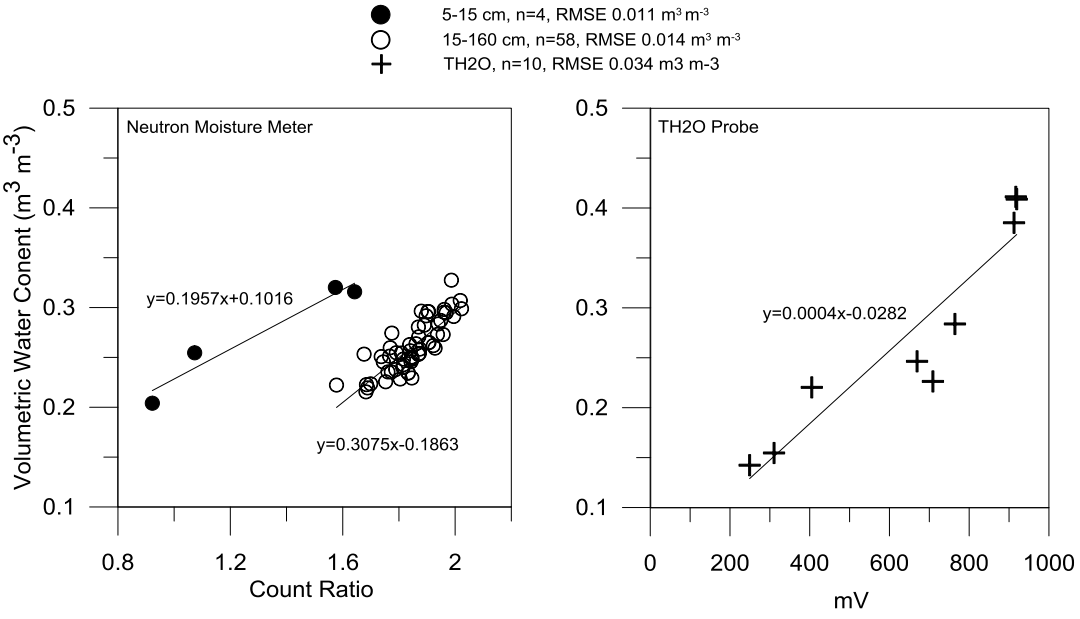

Figure 3.2. Calibration equations for NMM and TH2O probe on Burleson Clay.

Taking a NMM reading at the soil surface is not feasible because a significant portion of the neutron cloud would be occupied by air and many neutrons would escape

into the air. For this reason, NMM readings were taken no closer to the soil surface than 10 cm. At the soil surface, soil moisture was measured using a Delta-T Devices TH_2O Portable Soil Moisture Probe (Delta-T Devices, 2005). When the soil was dry, achieving good contact between the steel needles of the probe and the soil matrix was difficult. The TH_2O Probe was calibrated to volumtric soil water content on-site (n=10, $r^2 = 0.88$, RMSE = 0.034 $m^3 m^{-3}$;Fig. 3.2).

The representative soil area measured by the NMM is based on the size of the neutron cloud generated by the neutron source. The VWC calculation assumes that the area encompassed by the neutron cloud is soil and soil water. This assumption is less valid in cracked soils. Cracks impact the readings both when the cracks are filled with air (underestimation of VWC) and when the cracks are filled with water (overestimation of VWC), during or after precipitation events. The offset from the air filled cracks was accounted for by performing calibrations *in situ* with air-filled cracks present. Water-filled cracks are more difficult to account for because physical samples containing water-filled cracks and mesopores are impractical to take. These water-filled cracks and mesopores are a documented source of error in NMM measurements in which dry cracked soils are extensively and quickly wet (Jarvis and Leeds-Harrison, 1990; Fityus et al., 2011).

Changes in NMM readings in the presence of free water around access tubes have been estimated experimentally (Crespo, 2014) and simulated (Li et al. 2003). The annuluse size considered by measuremnet and simulation had a 0.95 cm wide cavity.These experiments used water filled annuluses around the NMM access tube in

heavy clay soils (Vertisols). Water-filled annulus are not the same as horizontal crackes filled with water. The author expecst that water filled cracks might have less of an effect than an annulus because of the geometry differences (Li et al. 2003). Crespo (2014) found that a water-filled gap around NMM access tubes in a Burleson clay soil increased NMM counts 1.1 times the count ratio in soils near field capacity. This finding by Crespo (2014) indicated a smaller influence in moist soils than simulated by Li et al. (2003). In drier soils, the influence of water-filled cracks on the NMM reading is expected to higher, 1.3 times the count ratio in soils near wilting point (Li et al. (2003)). Understanding the likely limits of this systamatic error improves interpretation of NMM readings under situations where there are water-filled cracks.

Depth of wetting, mass balance, and varibility of water content amoung tubes were considered for each irrigation event. For mass balance calcualtions, NMM readings for 10 to 120 cm depths on all ten access tubes were taken every 24 hours over four days in which no rain fell. These four readings allowed us to calculate profile mass balances of water for each access tube and compare the variability in this type of calculation. The depth of each soil layer was multiplied by the daily change in VWC to obtain the mm of water change for that layer. The change in water for each soil profile adjacent to a NMM access tube was the sum of the change in water for each soil layer in that profile. The same mass balance method was used to calculate the change in mm of water for the soil profile of each access tube during irrigation events.

PALMS Plot Simulations

The amount of irrigation added and the timing of the irrigation was recorded during each of the four irrigation events at the plot scale. This provided the precipitation data for PALMS simulations. For each set of precipitation data, two PALMS simulations were run, one with only Darcian flow (M&M module turned off) and one using two-domain flow (the M&M module on so that mesopores were present). Both PALMS simulations were given a clay soil texture for the entire profile depth (to 2.5 m). PALMS with M&M off used the Rawls et al. (1992) look-up tables, which are written in PALMS as default values, to obtain needed parameters with the exception of the value for field capacity water content. PALMS default field capacity water is 0.42 m^3 m^{-3} for a clay, but based on repeated NMM measurements, a field capacity water content of 0.44 m^3 m^{-3} was assigned.

The M&M module's nine parameters were chosen based on the official soil series description of a Burleson Clay (National Resource Consertvation Service, 2014) as interpreted by the Field Book for Describing and Sampling Soils (National Survey Center, 2002), with the exception of the COLE value, which was measured as 0.17 m m^{-1} by a previous study at this location (Neely, 2014). The saturated hydraulic conductivity of the ped ($K_{s,ped}$) was assigned the full Rawls et al. (1992) look-up table value of 0.06 cm hr^{-1} instead of 1/3 of the Rawls K_s recommended by Lepore (2009) because the shrink-swell activity of the soil inhibited clay film development and because the site was well structured for a Vertisol (Neely, 2014). The air entry potential, ψe was 0.370, Campbell's exponent for the moisture release equation (b) was 7.6, and the slit width at

field capacity ($2B_{ped}(\theta_{fc})$) was 0.006 cm, all of which are M&M module defaults developed from Rawls et al. (1992). Using the Burleson soil series description, h = 2, c = 26 cm, $w_{ped,0}(\theta_{fc})$ = 2 cm, and $w_{ped,max}(\theta_{fc})$ = 20 cm.

The VWC with depth predicted by PALMS simulations with and without the M&M module was compared to the average NMM VWC, at depth, for all five tubes in a plot for each sampling time during irrigation events. The RMSE and the Spearman's Rank correlation coefficient, as well as visual evaluation of graphs, are used to compare how well PALMS with the M&M module predicts VWC compared to PALMS without the M&M module. Additionally, the differences between simulated ponding for the M&M module on and off was considered in evaluating model performance.

PALMS Subwatershed Experiment and Simulations

Four PALMS simulations were run for a 4.4 ha watershed located in Riesel, TX at the Riesel Grassland Soil and Water Research Laboratory. Two simulations (one with the M&M module on and one with the M&M module off) were run for Years 2008, 2009 and 2010 using weather and precipitation data gathered for the watershed that is publically available online (USDA ARS, 2014). PALMS simulations were run with a 10 by 10 m grid cell spacing. M&M module parameters were the same as those used for the plot scale simulations.

The field is managed for improved grasses and rotationally grazed by cattle, on a Houston Black clay (Fine smectitic, thermic, Haplustert) that has less that has 0.01 m m^{-1} slope and chalk and marl parent materials. The topography for the watershed was measured using a survey quality GPS with ± 2 cm accuracy and a 1 by 1 m PALMS

input topography map was created from this data. NMM readings were taken at 20, 40, 60, 80, 100, and 120 cm depths on 5 locations at roughly two week intervals from July to December of 2008, from January to December of 2009, and from January to August of 2010. Measurements of VWC with the NMM and publically available runoff data (USDA ARS, 2014) were compared to PALMS output. Predictions of VWC, drainage at 120 cm, and runoff were compared for PALMS simulations with M&M module on and off.

Results and Discussion

Redistribution of Irrigation Water

Each 10 by 10 m plot was used twice; the first two irrigation events on the plots had drier initial water contents than the second two events. Figure 3.3 shows the average and standard deviation of volumetric water content for five NMM tubes at the beginning of each irrigation event. For each irrigation event and water content profile, the variability between tubes for the plot, the depth of wetting, and total change in profile water are discussed. In Figs. 3.3 to 3.6, the profile volumetric water content for each tube is shown over time. The wetting fronts for all tubes and all events are shown at two times, 2 hrs. (1.5 hrs. for Event 1) and 72 hrs. (24 hrs. for Event 4) after the start of the irrigation. For Events 1 and 2, the first volumetric water content profile for irrigation Events 3 and 4 are shown to provide an estimate of water content when it is certain that no free water is in the soil at the time of measurement. The wetting front was identified as the depth at which VWC at a given time after irrigation intersects initial water content

(hour 0 line). The wetting fronts for hour 2 and the final reading are summarized in Table 3.2.

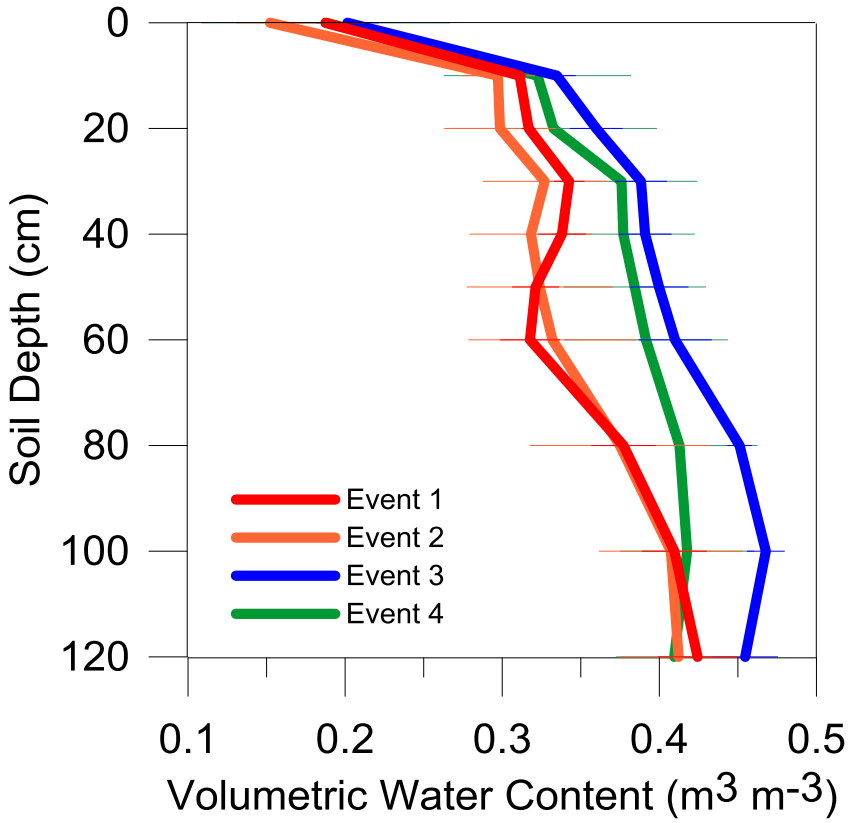

Figure 3.3. Initial soil volumetric water content for all irrigation events.

Events 1 and 4 were the higher intensity events and had all 22 mm of water applied in one hour. The intensity, duration, and amount of water were the same in Events 1 and 4, but the later started at a wetter initial water content (Fig. 3.3). Event 1 had a quick-moving wetting front in that water was detected at 120 cm by the initial 1.5-hr. soil water measurement. The wetter soil at 120 cm deep was detected in all five tubes

and stayed wetter after 24 hrs. of drainage. Event 4 also had a distinctly stable wetting front between the 2 hr. and final 24 hr. VWC measurement. However, the wetting front was shallower in Event 4 compared to Event 1. The deepest wetting front recorded for Event 4 was 70 cm, the average wetting front was 44 cm. Though both irrigation events began when cracks were visible at the surface, the drier soil in Event 1 had water moving via deeper subsurface cracks. Visual inspection of the VWC profiles and the mean VWC with standard error bars in Events 1 and 4 (Figs 3.4 and 3.7) shows that Event 1 had more variability among tubes. For example, the shape of the of the VWC profile at 2 hr. in Event 4 is consistent for all tubes, while in Event 1, a bulge in the wetting front around 60 cm that distorts the curve. Open preferential flow paths that narrow or terminate at this depth, causing temporary storage of free water in the cracks are likely the cause of such variability.

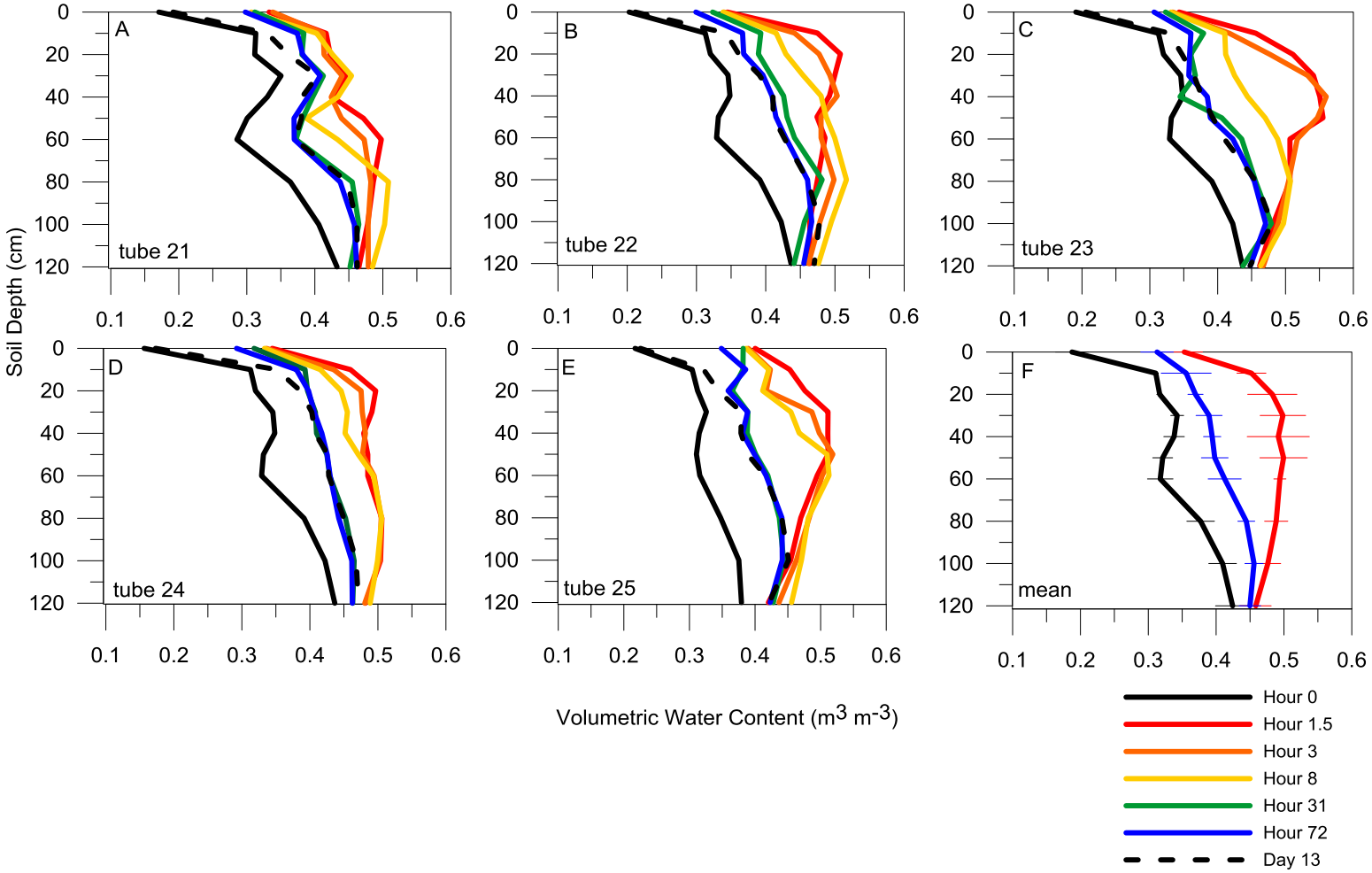

Figure 3.4. Profiles of volumetric water content (VWC) for all five neutron moisture meter tubes in Plot 2 during irrigation Event 1. Irrigation (22 mm) was only applied between hour 0 and 1.5. Plot F depicts mean VWC profiles for the five tubes at selected times and with standard deviation bars to illustrate natural variability in a plot.

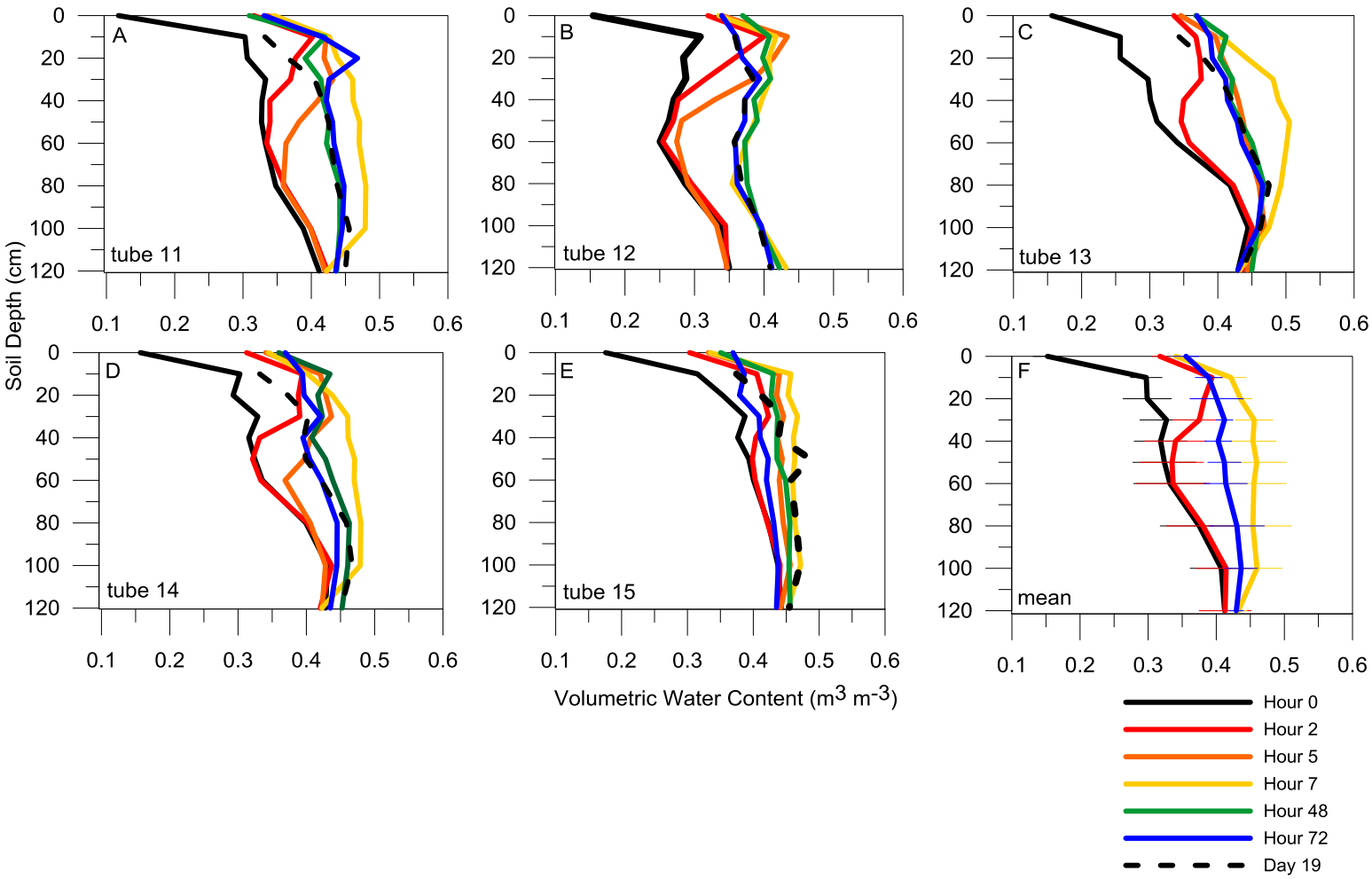

Figure 3.5. Profiles of volumetric water content (VWC) for all five neutron moisture meter tubes in Plot 1 during irrigation Event 2. Irrigation (22 mm) was applied between hour 0 and 2, 2 and 5, and 5 and 7. Plot F depicts mean VWC profiles for the five tubes at selected times and with standard deviation bars to illustrate natural variability in a plot.

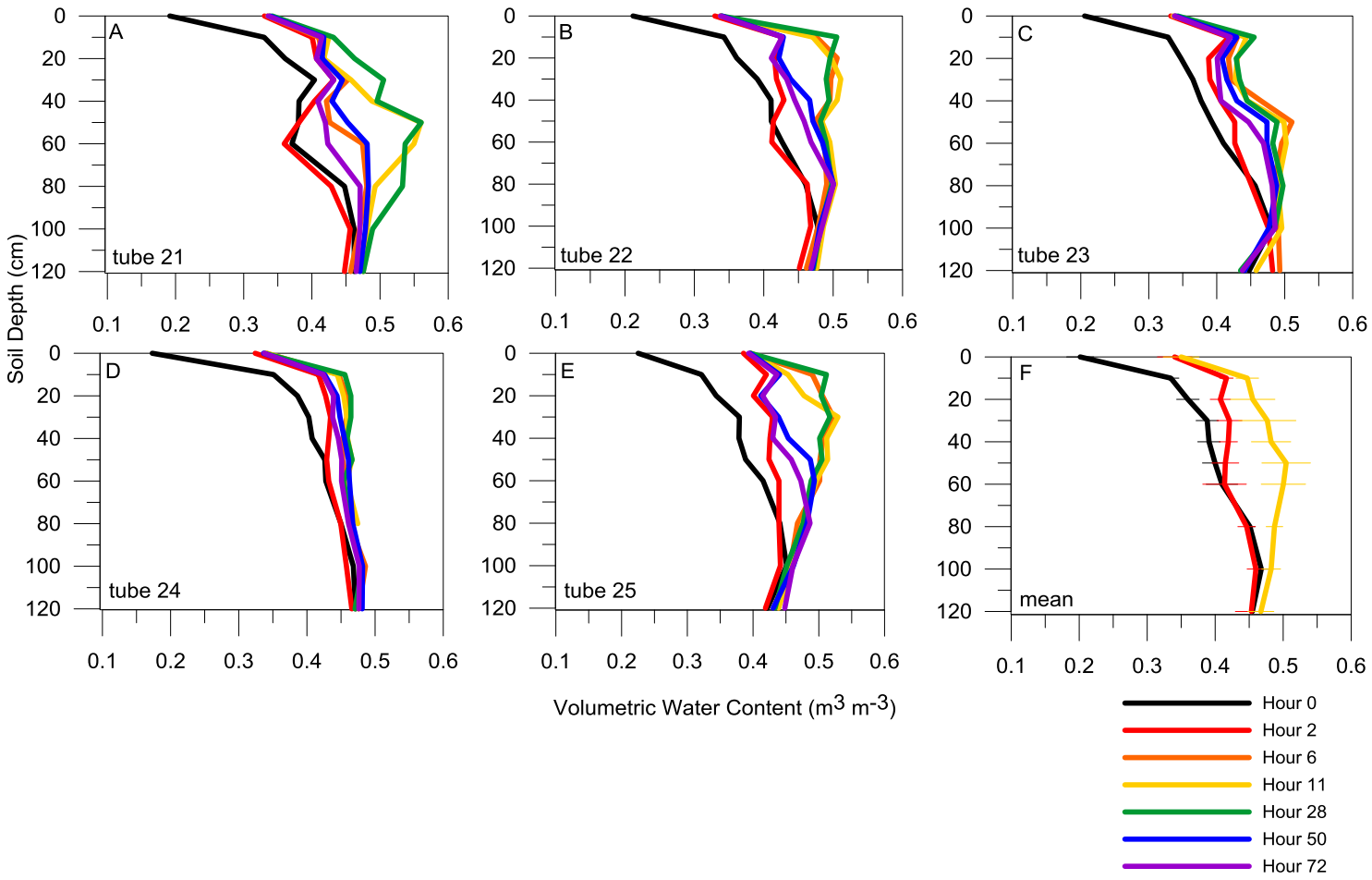

Figure 3.6. Profiles of volumetric water content (VWC) for all five neutron moisture meter tubes in Plot 2 during irrigation Event 3. Irrigation (22 mm) was applied between hour 0 and 2, and 2 and 6. Additionally, 11 mm was applied between hour 6 and 11 and also before hour 28. Plot F depicts mean VWC profiles for the five tubes at selected times and with standard deviation bars to illustrate natural variability in a plot.

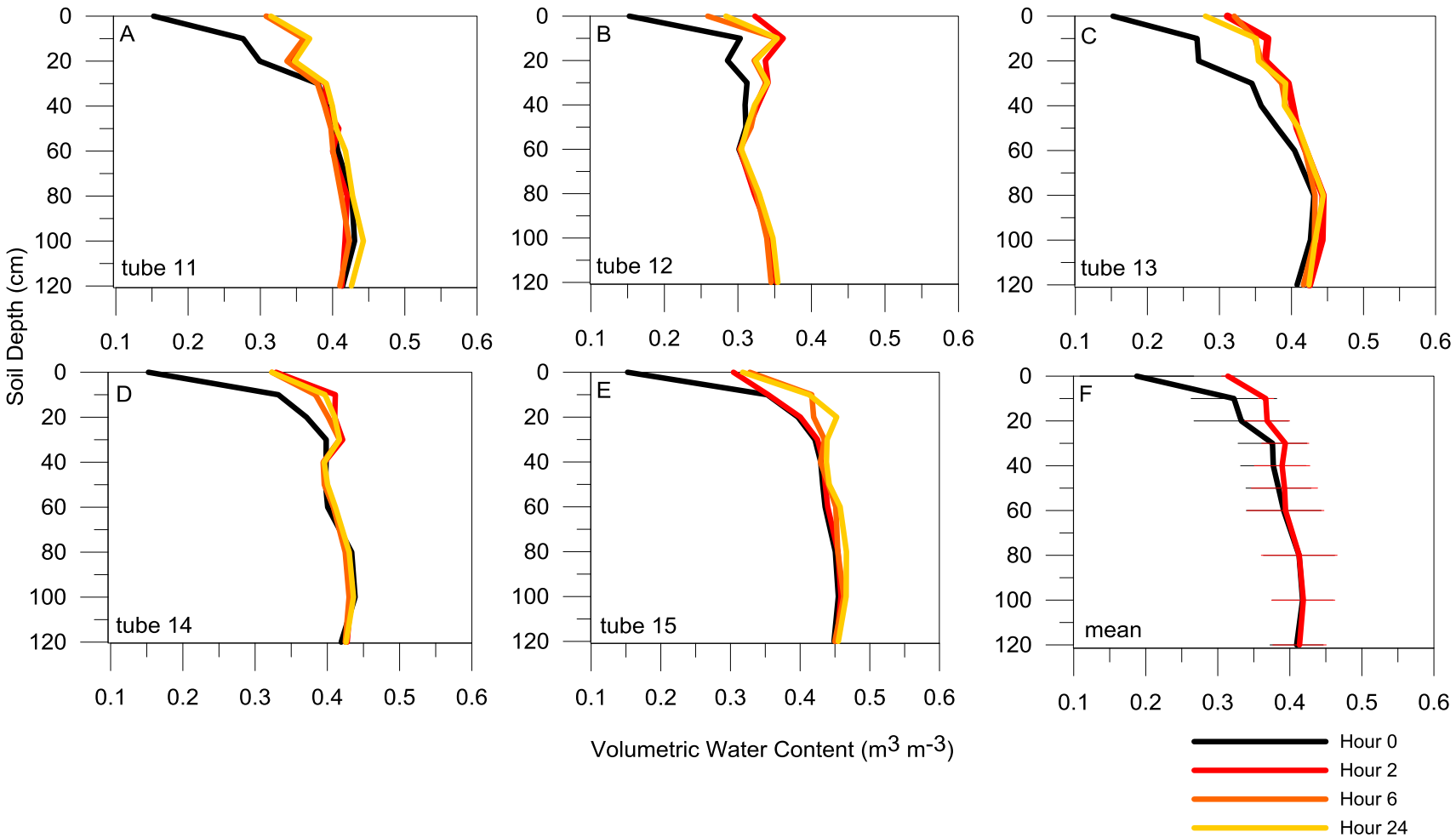

Figure 3.7. Profiles of volumetric water content (VWC) for all five neutron moisture meter tubes in Plot 1 during irrigation Event 4. Irrigation was applied (22 mm) between hour 0 and hour 1.5. Plot F depicts mean VWC profiles for the five tubes at selected times and with standard deviation bars to illustrate natural variability in a plot.

Table 3.2. Depth of wetting front in the soil profile 2 hours after irrigation began and final wetting front depth is shown. The volumetric water content (VWC) of the soil profile is shown for these same times.

Irrigation Event	Tube	Depth of Wetting cm	Profile Average VWC $m^3\ m^{-3}$	Depth of Wetting cm	Profile Average VWC $m^3\ m^{-3}$
		----------~2 hours----------		----------Final----------	
1	21	120+	0.44	120+	0.40
	22	120+	0.36	120+	0.41
	23	120+	0.36	120+	0.40
	24	120+	0.47	120+	0.41
	25	120+	0.46	120+	0.40
2	11	60	0.37	120+	0.43
	12	60	0.33	120+	0.38
	13	80	0.38	100	0.42
	14	50	0.37	120+	0.42
	15	50	0.40	100	0.41
3	21	50	0.40	100	0.42
	22	50	0.42	100	0.44
	23	80	0.42	100	0.43
	24	40	0.43	80	0.44
	25	80	0.42	100	0.44
4	11	30	0.39	30	0.39
	12	50	0.33	50	0.33
	13	70	0.40	70	0.39
	14	40	0.41	40	0.41
	15	30	0.40	30	0.44

Events 2 and 3 illustrate lower intensity irrigation events with drier and moister initial VWC profiles, respectively. Both Event 2 and Event 3 had lower intensities (17 mm hr^{-1} and 14 mm hr^{-1}, respectively) than Events 1 and 4. Events 2 and 3 were designed to simulate slower rainfall events that would thoroughly wet the soil, forcing mesopore flow, but not necessarily crack flow of water through the profile. Unlike Events 1 and 4, the wetting fronts of Events 2 and 3 continued to move deeper into the soil profile after 2 hrs. because irrigation continued for 8 and 24 hrs. for Events 2 and 3, respectively. In addition to this continued irrigation driving redistribution, the amount applied is greater (66 mm). On average both Events 2 and 3 had a wetting front to 60 cm deep at 2 hr. with only 10 cm of water added.

Tubes with a depth of wetting designated 120+ cm in Table 3.2 are assumed to have water drained past the last measured depth. Figure 3.4 indicates all measurement sites in Event 1 drained within 2 hrs of irrigation start. No other events drained in this short time range. The other initially dry event, Event 2, drained in 3 of 5 locations at 7 hrs. and 2 hours after that last irrigation began.

Event 1 is an especially good illustration of the speed that preferential flow paths introduce to the depth of redistribution of water in the top meter of a cracked soil. After 2 hrs., water had moved to a depth of 120 cm (and presumably deeper) as a result of mesopores/cracks routing water to that depth, and subsequently, wetting the soil. Soil has the highest VWC at 1.5 hr. indicating that water was infiltrating into cracks and afterward redistributing more slowly via mesopores and the soil matrix—for at least 8 hours. By the 31-hr. measurement, profile VWC is close to that of the 72 hr. and 13 d

measurements indicating water was out of the mesopores. It is also likely that VWC measured with the NMM while macropores contained water was an overestimation of water in the profile.

Neutron Moisture Meter Error Assessment

In light of the known interference that water in soil cracks has on NMM measurements, the over-estimation of the NMM counts were evaluated before comparing the NMM measurements to PALMS simulations. First, the difference in total water estimated for the soil profile around each access tube was calculated for before and after irrigation and compared to the amount of water added. Basically, if the NMM method is accurate, the amount of water change in the profile would be roughly equal to the amount added by the sprinklers. Before comparing the differences in water, the NMM-estimated change in VWC was calculated over four days in which no water was applied and for all ten access tubes used in the experiment. NMM readings were taken once daily from 15 to 18 July, 2013. The change in volumetric water content from 15 July, for each soil layer was multiplied by the thickness of each soil layer in the profile and summed to yield mm of water change for 16, 17, and 18 July. The water change across for all soil layers was calculated for each tube individually. If this mass balance method is precise, the change in water should be equal to the water lost by soil evaporation only (Table 3.3).

Table 3.3. Change in water content in the soil profile surrounding ten access tubes over four days with no precipitation or irrigation.

Tube ID	Water Change	Tube ID	Water Change
	mm		mm
	July 16th, 2013		
11	-5	21	-9
12	-7	22	-5
13	-36	23	-5
14	-4	24	-2
15	29	25	-2
	July 17th, 2013		
11	13	21	12
12	15	22	21
13	33	23	29
14	16	24	30
15	-6	25	18
	July 18th, 2013		
11	1	21	-9
12	3	22	-29
13	4	23	-6
14	6	24	-24
15	21	25	18
min	-36	min	-29
max	33	max	30
mean	6	mean	3

Based on the mass balance calculations, both plots gained water, 3 and 6 mm on average, though no rain fell. No tube showed either loss of water every day or water added every day. There was a slight daily trend of overall loss of water day 16 July, gain of water on day 17 July, and no clear trend 18 July. As much as 36 mm was lost from the 1.4 m profile according to this mass balance approach while a three-day first stage energy limited evaporation would be 6 mm per day if the surface soil were very wet (Ritchie, 1972). Even more unreasonable is the addition of 33 mm from 16 to 17 July in tube 13. Based on this mass balance for access tubes when no water was applied (assuming no evaporation) the RMSE of this approach is 17 mm.

Table 3.4 provides the results of the mass balance of water for each measurement time and irrigation event. On average, the water balances indicate gains in soil water storage beyond that which was irrigated in Events 1, 2, and 4, while the soil profiles of Event 3 lost water. The average changes in mm of water beyond the amount irrigated over the entire measurement period were +85, +21, -53, and 33 mm for Events 1 through 4, respectively. Clearly and as expected, early in the infiltration event the two dry soils had the highest overestimation of water (Table 3.4). Interestingly, low initial soil moisture, rather than amount and intensity, had the higher water gains from the mass balances.

Higher gain at lower water content is likely in part because water filled cracks will influence the NMM measurements more when the soil matrix is drier (Li et al., 2003). Event 4 had the same irrigation intensity as Event 1, but moist initial water contents, and had a lower overestimation of water by the NMM measurements. Event 1,

which is suspected to have had the most preferential flow activity based on the examination of the depth and time of wetting, had an average gain of 53 mm of water in the soil profile at 72 hrs., which is about 3 times the RMSE of the mass balance approach. Events 2 and 4 had average gains in profile water that were within the range of the uncertainty of the mass balance approach (the largest gain in the non-irrigated measurements was 33 mm). Event 3, which lost water, lost more water than what was observed in the non-irrigated measurements. The author's mass balance approach, though highly uncertain, detected preferential flow in Event 1, when many cracks were open and water was applied at high intensity.

The mass balance of water in soil profiles before and after irrigation indicated the need for a field experiment that sought to quantify the interference that water filled cracks have on the volumetric water content measured by the NMM. Addressing the problem of water-filled cracks is difficult experimentally and mathematically, in that the geometry of cracks around the NMM access tube is not well understood. The fraction of crack volume filled with water would have to be known as well. Rather than find exactly how much to adjust a NMM count ratio for a particular access tube at a particular state, the author sought to bound the influence of water-filled cracks on the NMM count ratio.

Table 3.4. Change in water content of the soil profile surrounding access tubes (minus water applied to plots). If the neutron moisture mass balance approach was accurate the values should be zero.

	Soil Profile Water Minus Irrigation water (mm)						
	tube #	1	2	3	4	5	Average
Event 1	hour 1.5	118	116	158	126	126	129
dry	hour 3	112	117	140	119	119	121
	hour 8	114	116	101	108	108	109
	hour 31	69	65	45	61	61	60
	hour 72	61	53	42	56	56	53
	day 13	47	45	34	35	54	43
Event 2	hour 2	-17	-26	-5	-26	-32	-21
dry	hour 5	11	-4	45	7	-2	11
	hour 7	82	65	79	56	19	61
	hour 48	43	68	48	42	2	41
	hour 72	51	47	37	21	-27	26
	Day 19	10	27	15	-1	-11	8
Event 3	hour 2	-45	-43	-26	-38	-38	-38
wet	hour 6	-8	9	15	-11	-11	-1
	hour 11	9	7	10	-4	-4	4
	hour 28	50	3	5	-9	-9	8
	hour 50	1	9	-8	-13	-13	-5
	hour 72	-18	-28	-17	-21	-21	-21
Event 4	hour 2	1	12	36	9	-3	11
wet	hour 5	-1	-1	26	1	9	7
	hour 24	16	6	27	8	18	15

Table 3.5. Volumetric water content of the soil and associated over estimate of volumetric water content using the neutron moisture meter with a 0.95 cm water-filled annulus around the access tube.

Volumetric Water Content, $m^3\ m^{-3}$							
Actual Soil Moisture	0.28	0.32	0.36	0.40	0.44	0.46	0.48
Simulated*	0.44	0.50	0.50	0.55	0.57	0.59	0.61
Measured*					0.49	0.50	

* Simulated values are estimated from Li et al. (2003); measured values are experimentally measured and found in Crespo (2014).

Table 3.5 was created to estimate an upper bound of overestimation by the NMM for soils at VWC of 0.28 to 0.48. Because the author expects that the access tubes were not completely surrounded by a water-filled annulus and cracks were filled partially with air (which would lower count ratios), and the crack geometry is different from annulus geometry, the worst case over estimation by the NMM, would be less than 0.16 $m^3\ m^{-3}$ for the drier soil (0.28 $m^3\ m^{-3}$) and less than 0.05 $m^3\ m^{-3}$ at the mean water content of 0.40 $m^3\ m^{-3}$.

To assess error tolerance of this experiment, the author compared the uncertainty caused by water in soil cracks to the variability between tubes in a plot. The highest standard deviation for Plot 1 across all events has an average of 0.04 $m^3\ m^{-3}$ and ranges from 0.08 to 0.005 $m^3\ m^{-3}$. The average standard deviation between water contents of the five tubes in Plot 2 was 0.02 with a range of 0.09 to 0.004 $m^3\ m^{-3}$. In summary, the overestimation of soil moisture in water-filled cracks ranges from 0.06 to 0.16 $m^3\ m^{-3}$ (always a positive bias) and the plot variability from 0.02 to 0.04 $m^3\ m^{-3}$. Additionally, by comparing +24-hour, post-irrigation, soil water measurements to 19-day post irrigation, the author is confident that NMM measurements of soil water after 24 hours is

primarily a function of soil matrix water only. Information provided in soil water measurements measured prior to 24 hrs. post irrigation will be interpreted with known biases and plot variability in mind.

PALMS Plot Simulations

The primary difference between PALMS infiltration and redistribution of water with the M&M module on and off is that the M&M module moves water more quickly down the soil profile, allowing water to infiltration and drain, whereas when the M&M module is off, water redistribution is governed by Richards' equation which slowly redistributes water and the Green and Ampt infiltration estimate causes ponding in high intensity rainfalls. PALMS with the M&M module on had no ponding in any of the simulations. PALMS without the M&M module ponded water on the soil surface in every simulation. In the plot, ponding of water was only observed during Event 3. Occurrence of ponding in the simulations, and subsequent runoff, resulted in drier VWC deeper in the soil profile and saturated surfaces. The soil surface thoroughly wets because the Richards equation requires Darcian wetting of the matrix. With the M&M module on, the one-hour period in which water was applied by irrigation was the only time available for peds to absorb water from surrounding mesopores. Hence the soil wet deeper but the surface did not saturate as water bypassed the surface and moved in response to gravity. With the M&M module on, cumulative drainage of water at 120 cm depth ended within the 15 minute time step after irrigation and totaled 14.8, 52.2, 52.8 and 14.2 mm for Events 1, 2, 3 and 4. VWC as measured by NMM readings per plot and all irrigation events are graphed along with predicted VWC for PALMS (Figs.3.8-3.11).

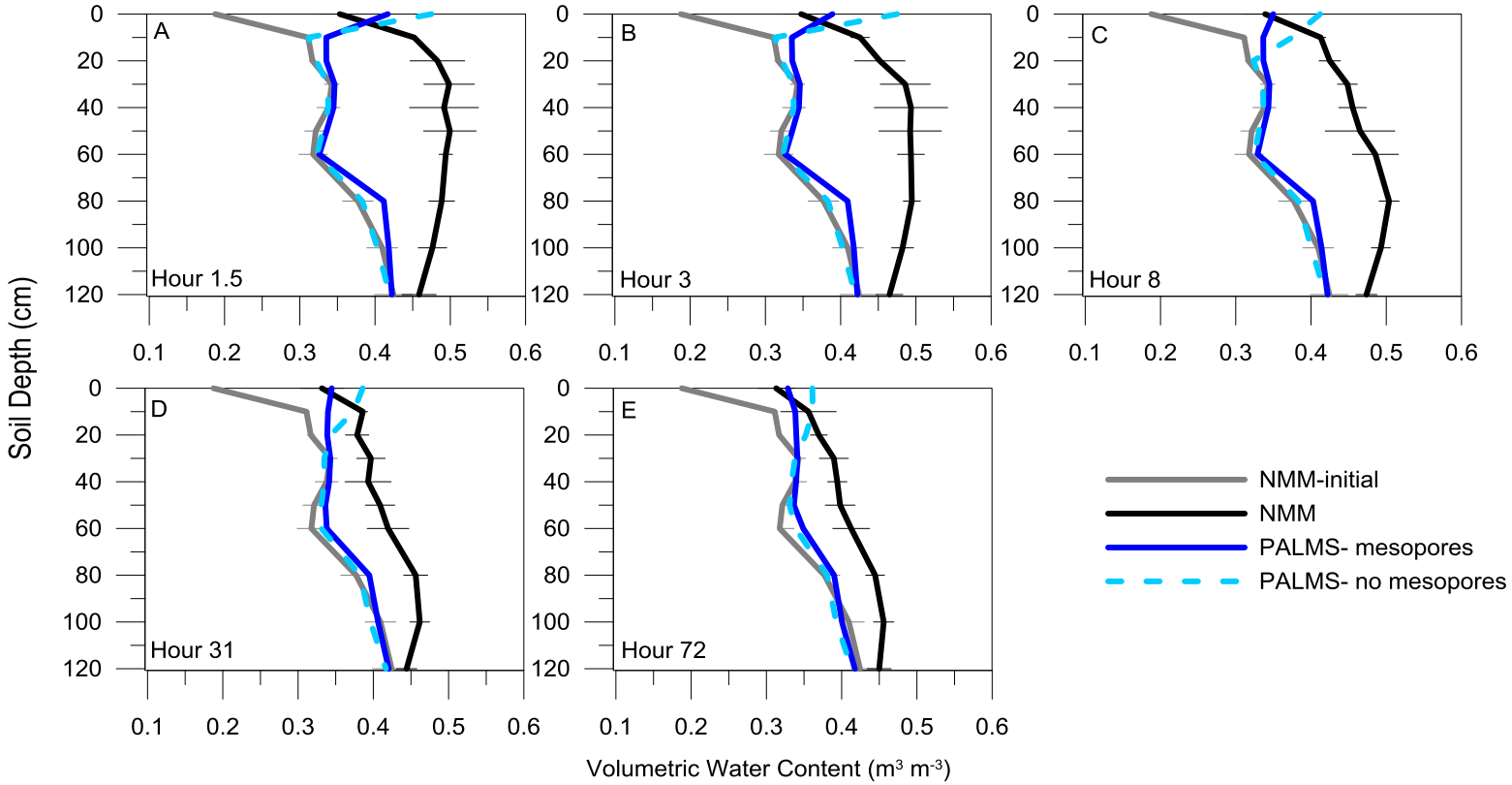

Figure 3.8. Volumetric water content with depth for PALMS simulations with and without mesopores and mean of all 5 neutron moisture meter (NMM) readings with standard deviation bars during irrigation Event 1. Irrigation (22 mm) was only applied between hour 0 and 1.5.

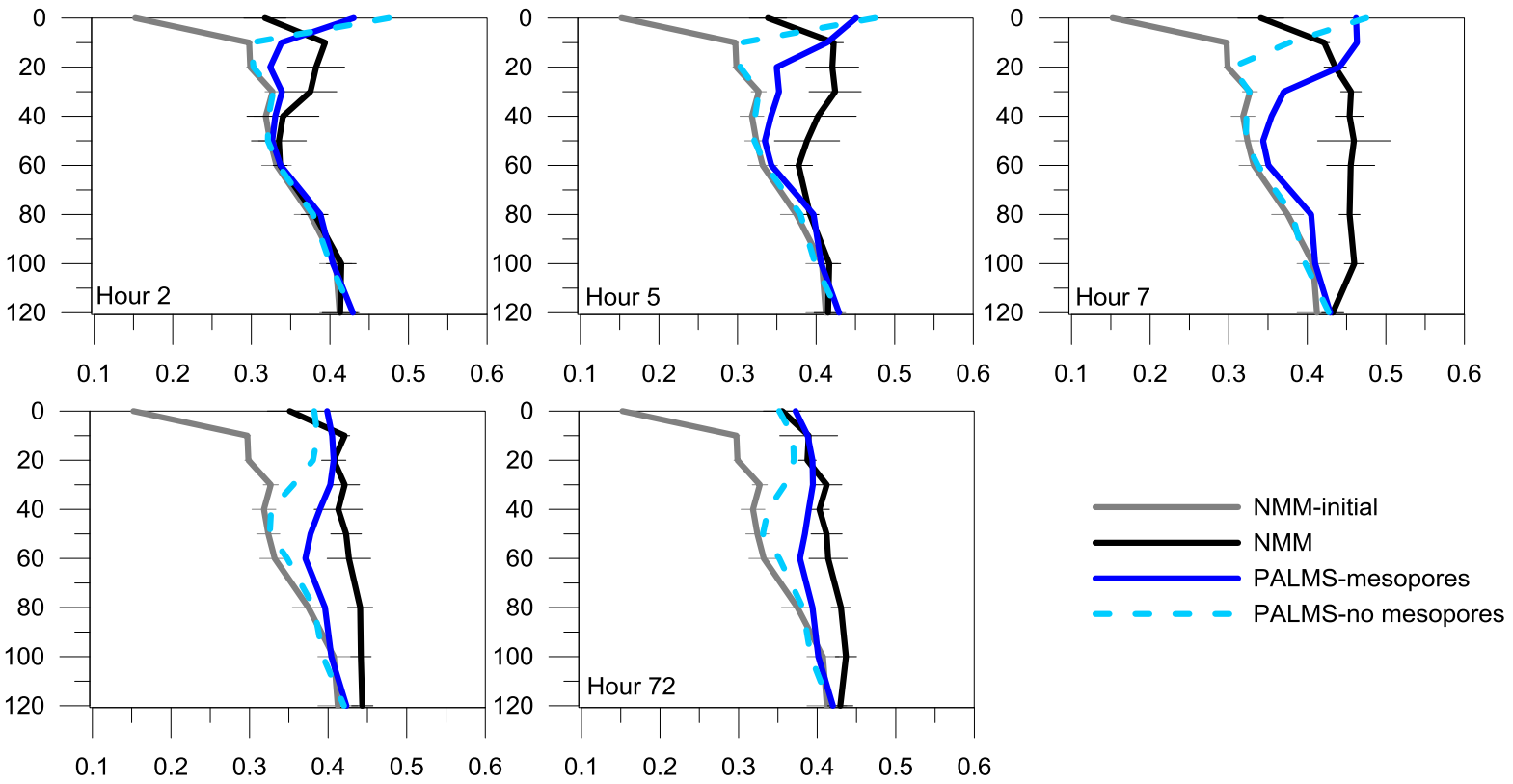

Figure 3.9. Volumetric water content with depth for PALMS simulations with and without mesopores and mean of all 5 neutron moisture meter (NMM) readings with standard deviation bars during irrigation Event 2. Irrigation (22 mm) was applied between hour 0 and 2, 2 and 5, and 5 and 7.

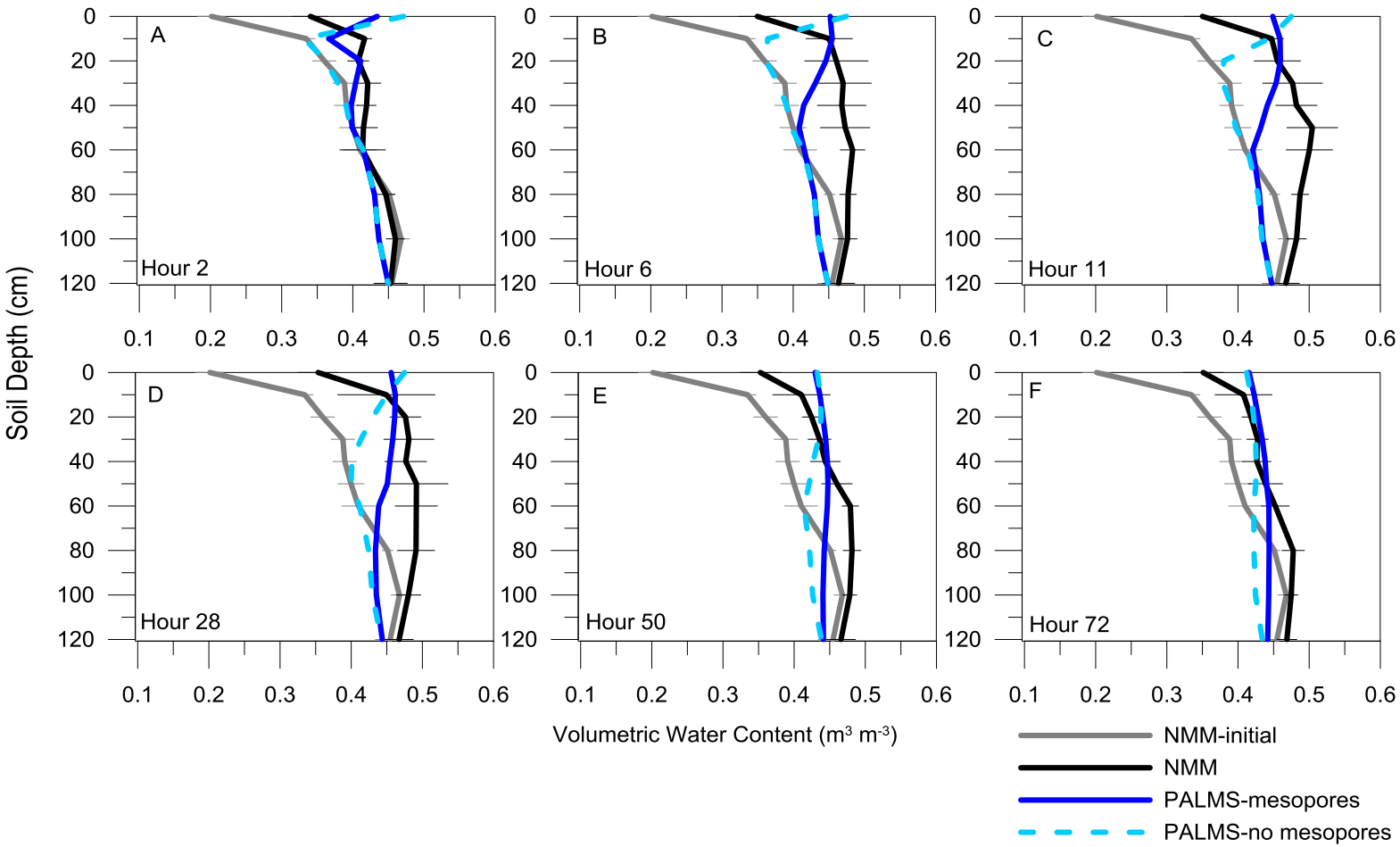

Figure 3.10. Volumetric water content with depth for PALMS simulations with and without mesopores and mean of all 5 neutron moisture meter (NMM) readings with standard deviation bars during irrigation Event 3. Irrigations (22 mm) was applied between hour 0 and 2, and 2 and 6. Additionally, 11 mm was applied between hour 6 and 11 and also before hour 28.

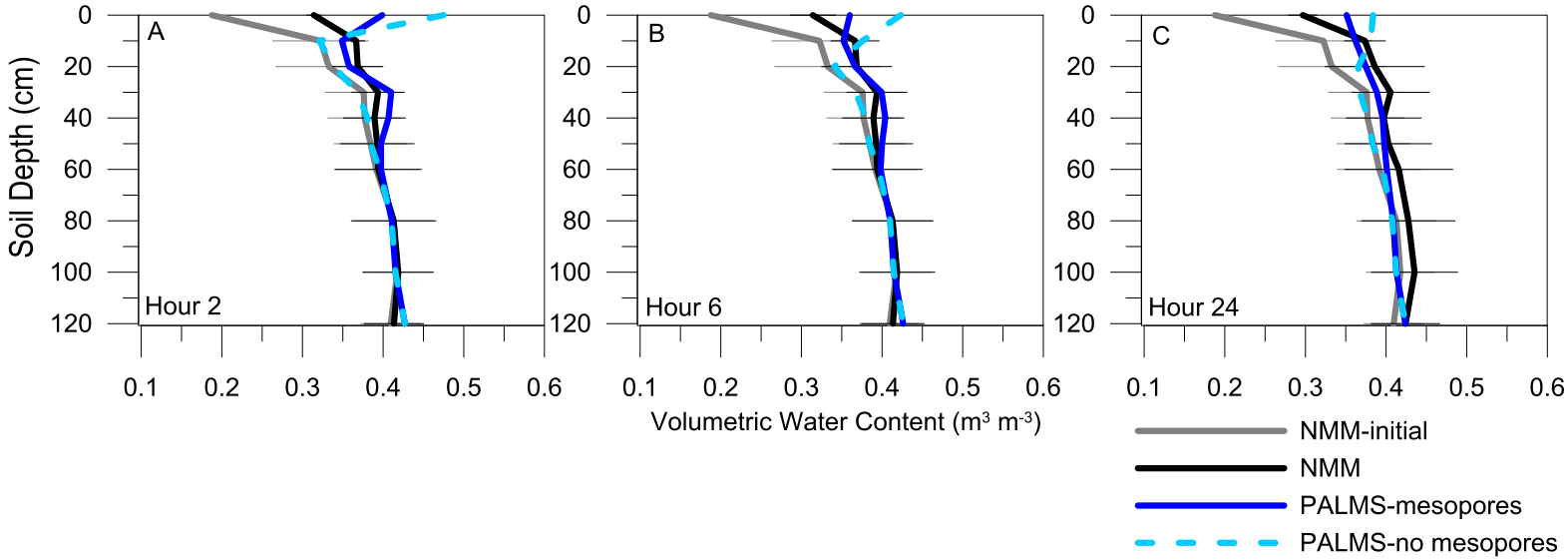

Figure 3.11. Volumetric water content with depth for PALMS simulations with and without mesopores and mean of all 5 neutron moisture meter (NMM) readings with standard deviation bars during irrigation Event 4. Irrigation was applied (22 mm) between hour 0 and hour 1.5.

In Event 1, there is not a striking difference between the profile VWC modeled by PALMS with M&M module on versus off. With the M&M module off, Richards' equation wets the soil more at the surface and water does not move past 30 cm after 72 hrs. The M&M module shows some wetting at depth (55 to 80 cm at 72 hrs) and at 72 hrs. agrees well with measured VWC at the surface (Fig. 3.8). However neither PALMS simulation matched the measurement of VWC very well. The water ran off the plot with Richards' equation governing water flow, and drained with M&M module governing flow. Ideally the M&M module needs to have blocked mesopores to allow the water to laterally infiltrate into the soil peds. The 72 hr. VWC measurement is likely more representative of how much water actually infiltrated into the soil matrix and how much drained. However the mass balance still shows 53 mm of excess water. Spread out over 130 cm of soil creates an estimate of $0.04 m^3\ m^{-3}$ over estimation of water content by the NMM, assuming no drainage. Accounting for this potential over estimate gets the simulations within the variability of the plot, but the simulation results don't differ in VWC. The RMSE values are high and similar, the correlation coefficients are better for M&M Module on, but not encouraging (Table 3.6).

A clearer picture emerges of the M&M module increasing soil VWC at depth in Event 2. Like Event 1, the soil was initially dry, but more water was applied more slowly ($17\ mm\ hr^{-1}$) in Event 2. Here it is obvious as previously discussed that in hrs. 2 through 7 the NMM measurements are being influenced by water in soil cracks and mesopores. The wetting front simulated by PALMS with M&M module is similar to the NMM at hr. 7, however, in the end the soil actually wet to 120 cm and PALMS with M&M on wet

the soil to 80 cm. Again, the fault of the M&M module was that the water drained too quickly to allow the clay soil with a low hydraulic conductivity to adsorb the water. If getting the water deeper in the soil profile is of primary importance, the M&M module performed better. The RMSE of the M&M model with respect to measured VWC was much better than when the M&M module was turned off, 0.02 versus 0.05 m^3 m^{-3}, respectively at 72 hrs (Table 3.6). Correlation coefficients comparing the general trends of VWC profile characteristics varied with no clear, better choice.

Table 3.6. Root means square error (RMSE) and Spearman's rank correlation coefficient (d) for predictions of volumetric water content for all Events with M&M on and off.

			Event 1				
Hour	0	1.5	3	8	31	72	
RMSE M&M off	0.01	0.14	0.13	0.11	0.06	0.05	
RMSE M&M on	0.01	0.13	0.12	0.10	0.06	0.05	
d M&M off	0.98	-0.10	0.33	0.42	0.40	0.50	
d M&M on	0.98	-0.22	0.10	0.37	0.55	0.77	
			Event 2				
Hour	0	2	5	7	48	72	
RMSE M&M off	0.01	0.05	0.07	0.10	0.06	0.05	
RMSE M&M on	0.01	0.03	0.04	0.07	0.03	0.02	
d M&M off	0.98	0.33	-0.25	-0.15	0.52	0.50	
d M&M on	0.98	0.63	0.50	-0.68	0.05	0.50	
			Event 3				
Hour	0	2	6	11	28	50	72
RMSE M&M off	0.01	0.04	0.05	0.06	0.05	0.04	0.03
RMSE M&M on	0.01	0.04	0.05	0.06	0.05	0.04	0.01
d M&M off	0.98	0.63	0.55	-0.08	-0.92	-0.65	0.38
d M&M on	0.98	0.56	-0.72	-0.91	-0.53	0.34	0.94
			Event 4				
Hour	0	2	6	24			
RMSE M&M off	0.01	0.02	0.01	0.02			
RMSE M&M on	0.01	0.01	0.01	0.01			
d M&M off	0.95	0.93	0.90	0.78			
d M&M on	0.95	0.90	0.78	0.90			

Event 3 has the same intensity and amount of water applied as Event 2, but measured initial VWC was wetter than Event 2. Notably, measured initial VWC was higher than field capacity (0.44. $m^3 m^{-3}$) in PALMS. Because initial VWC was higher than field capacity set in PALMS, PALMS immediately started draining water out of the bottom, resulting in marginally lower simulated water contents below ~70 cm (Fig. 3.9). Event 3, like Event 2 shows the M&M module moving water deeper more quickly in the first 24 hrs., but by 72 hrs., the simulation results with M&M module off are not very different. The RMSE values of the two simulations compared to measure VWC are nearly identical, the M&M module underestimates VWC in the top 30 cm and VWC with M&M module off underestimates below 40 cm (Fig. 3.10 and Table 3.6).

Event 4 has the same amount of water added as Event 1, but water is applied to a soil that was wetter at the start of irrigation. The M&M module moved water to depth more quickly and did not pond water. The wetting front of the M&M module matched measurements from 2 and 6 hrs. Overall, PALMS simulations with the M&M module on worked well and better than PALMS with the M&M module off (Fig. 3.11 and Table 3.6)

The RMSE values consistently favor running PALMS with M&M module on, while the Spearman's correlation indicates better pattern fit with VWC values with M&M Module off, especially, earlier in the irrigation events, because the ponding resulted in surface volumetric water contents that are closer to the range of those measured. The Spearman's coefficients after 24 hrs. indicate that the simulated VWC

pattern with M&M module on correlates better to measurements, because the soil surface has drained a bit more.

PALMS Subwatershed Simulations

The same model behaviors observed at the plot scale were seen when PALMS with M&M module on and off were compared to NMM measurements of soil profile VWC on a 4.4 ha field. Figures 3.12-3.14 depict average NMM measurements with standard deviation bars across five locations in the field and PALMS-simulated VWC at six soil depths for three years, 2008, 2009, and 2010.

In Figures 3.12-3.14, it is visually confirmed that the M&M module allows water to move deeper in the soil profile. The most striking example of this is in 2009, which received more rainfall (1115 mm yr^{-1}) than either 2008 or 2010, 690 and 563 mm yr^{-1}, respectively. Any improvement in simulating soil water content by using the M&M module is evaluated in Table 3.7, which gives the RMSE and Spearman's Rank correlation coefficient (d) for the sixth soil depths for each year. When the M&M module was on, simulated soil water content was more strongly correlated to measured water contents in general. The M&M module had smaller RMSE values only in 2008, and had the worst RMSE values in 2009, the same year in which the patterns of soil moisture were most strongly correlated to the soil moisture measurements. The RMSE values are primarily evaluating model goodness for when the soil is drier because that is when the majority of soil moisture measurements were made. If the M&M module is getting water deeper into the soil profile, it should be generally wetter (Figs. 3.12 to 3.14). Hence the poor RMSE values in 2009 are a result of the M&M module having

wetter soil and the PALMS subroutine that estimates evapotranspirtaion did not pull as much water out deeper to dry down the soil on days 150 to 250 (Fig. 3.13).

While the volumetric water content modeled by PALMS when the M&M module is on and when the M&M module is off are not drastically different, the two approaches partition drainage and runoff very differently. When the M&M module was used, no water ponded or ran off in any of the three years. All simulations had runoff when the M&M module was turned off and the Richards equation governed water movement through the soil. In Figure 3.15, runoff measurements from the sub watershed (SW17) in 2008 and 2009 are compared with runoff predictions from PALMS with M&M module off. It is clear that PALMS without the M&M module over-predicts runoff in both years (2010 runoff data was unavailable), with the largest runoff event in 2009 being modeled more than six times larger than it was measured.

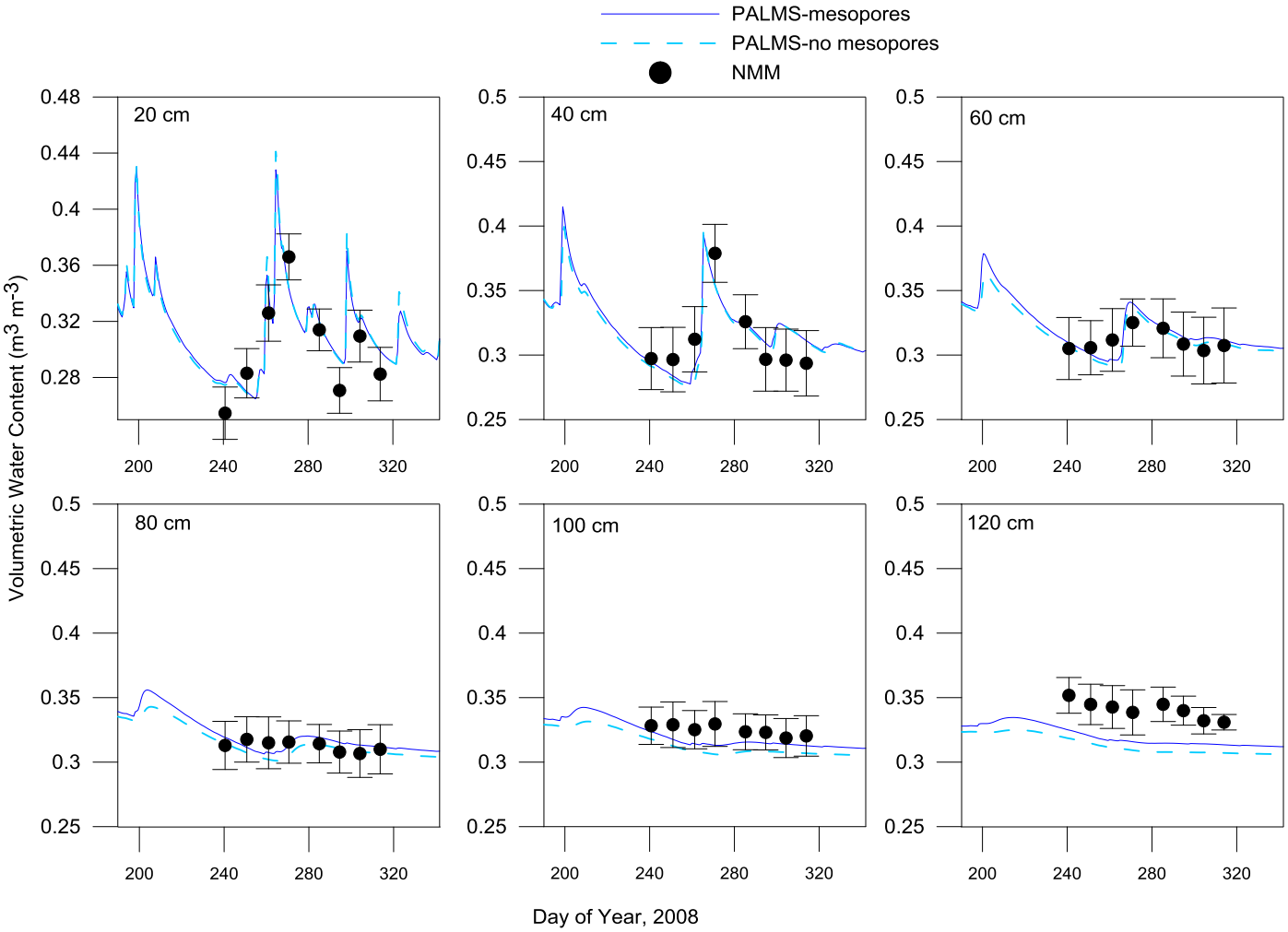

Figure 3.12. Volumetric water content with depth for PALMS simulations and neutron moisture meter (NMM) on field SW17 at Riesel, Texas in 2008.

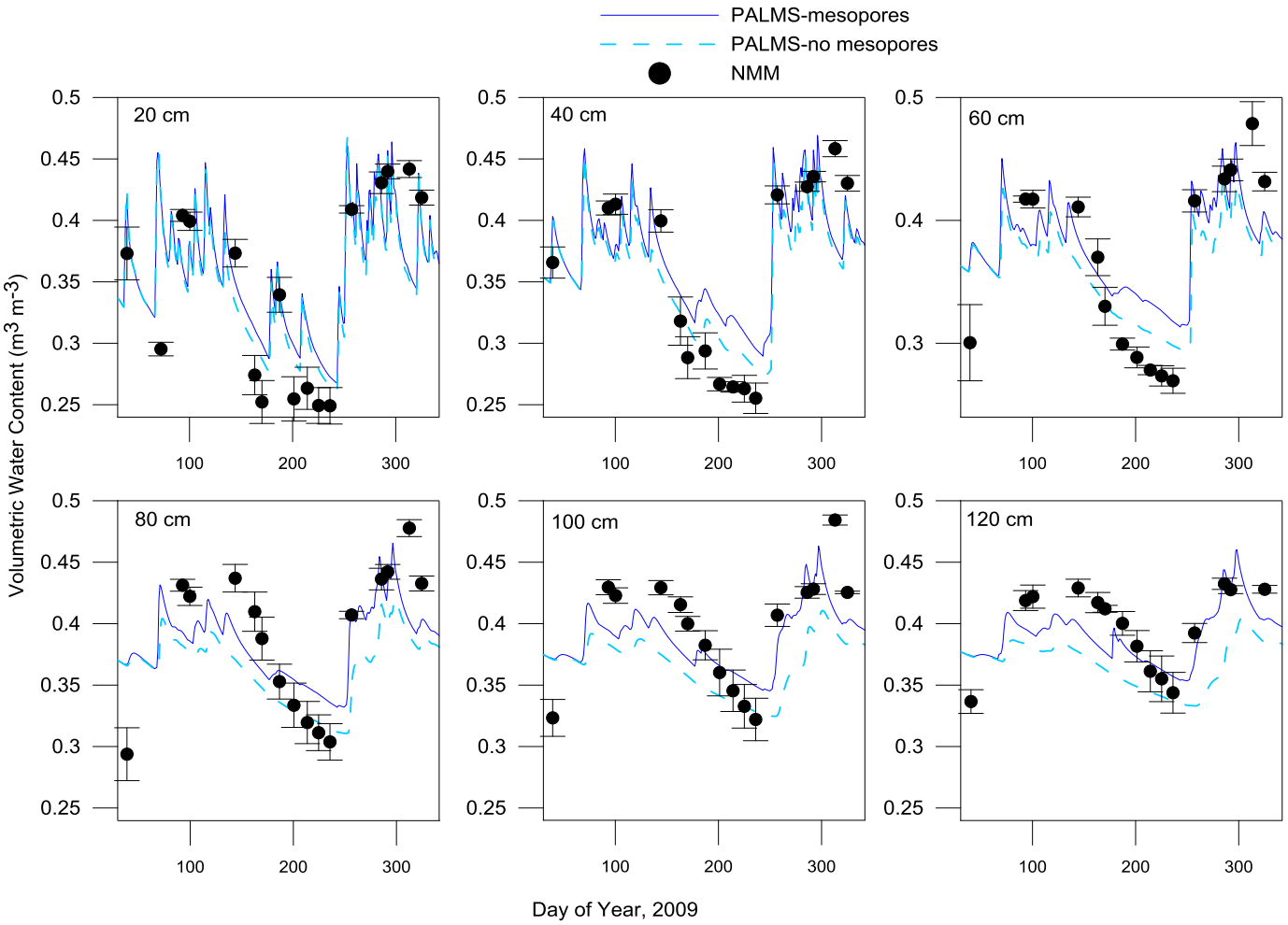

Figure 3.13. Volumetric water content with depth for PALMS simulations and neutron moisture meter (NMM) on field SW17 at Riesel, Texas in 2009.

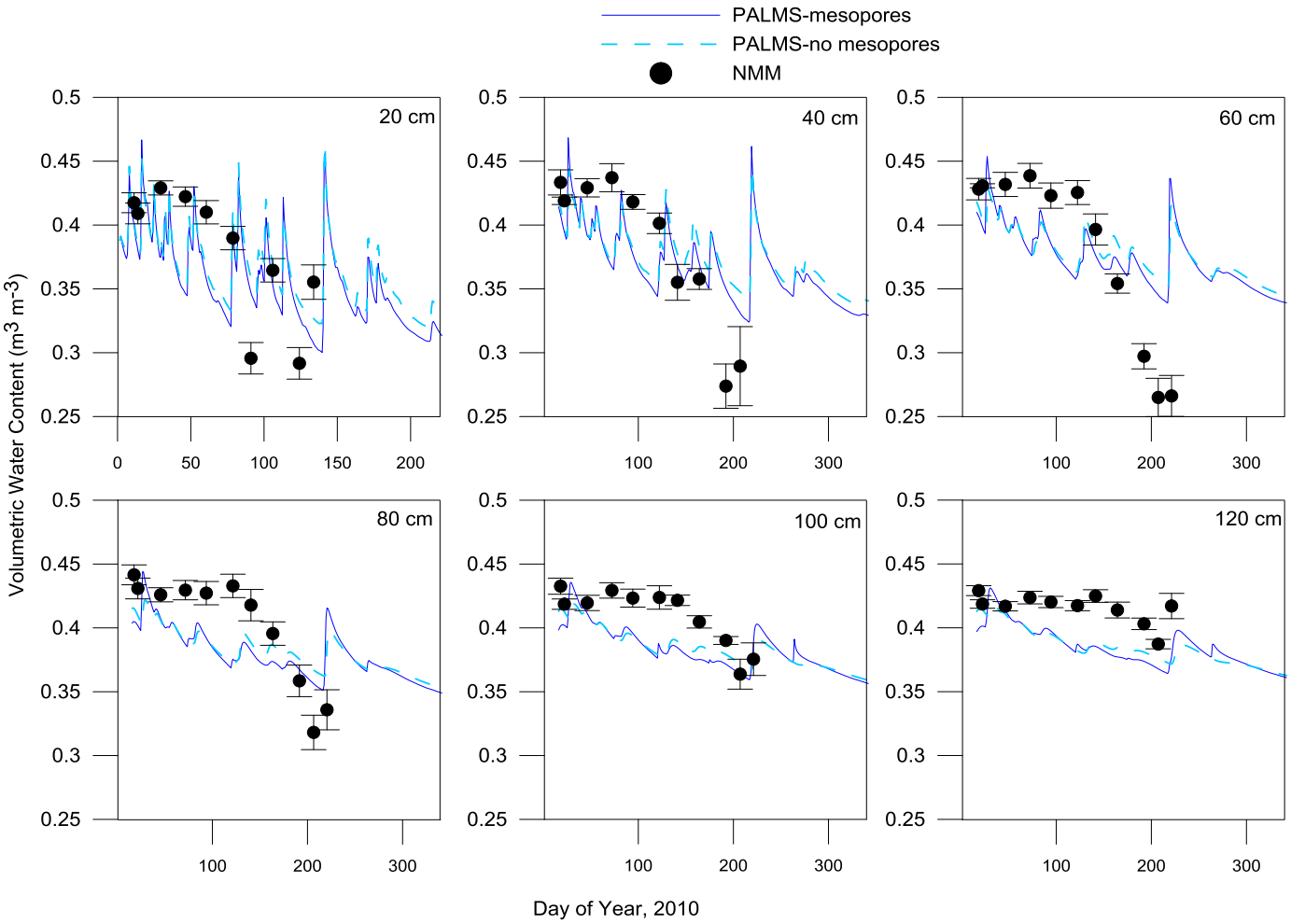

Figure 3.14. Volumetric water content with depth for PALMS simulations and neutron moisture meter (NMM) on field SW17 at Riesel, Texas in 2010.

Table 3.7. Root means square error (RMSE) and Spearman's correlation coefficient (d) for predictions of volumetric water content made by PALMS with M&M on and off for 2008, 2009, and 2010.

			2008				Mean RMSE
Soil Depth	20cm	40 cm	60cm	80cm	100cm	120cm	
RMSE M&M off	0.018	0.020	0.009	0.007	0.016	0.031	0.017
RMSE M&M on	0.017	0.017	0.009	0.006	0.010	0.024	0.014
d M&M off	0.81	0.26	0.48	-0.40	0.19	0.81	
d M&M on	0.83	0.33	0.48	-0.31	0.36	0.81	
			2009				
Soil Depth	20cm	40 cm	60cm	80cm	100cm	120cm	
RMSE M&M off	0.047	0.108	0.109	0.105	0.098	0.130	0.100
RMSE M&M on	0.048	0.110	0.112	0.108	0.102	0.134	0.102
d M&M off	0.66	0.68	0.66	0.59	0.59	0.39	
d M&M on	0.65	0.67	0.69	0.67	0.70	0.78	
			2010				
Soil Depth	20cm	40 cm	60cm	80cm	100cm	120cm	
RMSE M&M off	0.069	0.071	0.066	0.036	0.024	0.026	0.049
RMSE M&M on	0.070	0.070	0.067	0.041	0.026	0.029	0.050
d M&M off	0.08	0.18	0.24	0.60	0.64	0.65	
d M&M on	0.11	0.22	0.41	0.35	0.52	0.56	

When the M&M module is used in PALMS, runoff is under predicted (there is no runoff modeled), rather all rainfall infiltrates into the soil. Infiltration is either captured by the soil or drains through the soil profile. Because the NMM measurements extend to 120 cm, the authors has chosen to evaluate the drainage and water retention for the soil profile from 0-120 cm depth. When the M&M module was used, drainage essentially doubled in each year. In 2008, the M&M module increased the predicted drainage from 6-9 to 64 mm, in 2009 from 86-100 to 287 mm, and in 2010 from 50-58 mm to 118. The drainage in PALMS with M&M module off varies because runoff routs water around the field. In addition to draining more water, PALMS with the M&M module captured more water in the top 120 cm the soil profile in each year, 7, 10 and, 15 mm in 2008 to 2010, respectively. Though no drainage measurements are available for the site, the drainages is likely too great because the amount of water that the M&M module redirected from runoff (Fig. 3.15) is much greater than the resulting increase in soil water stored (roughly 10 mm per year). In other words, it seems that the M&M module does not allow enough water to get into the soil matrix.

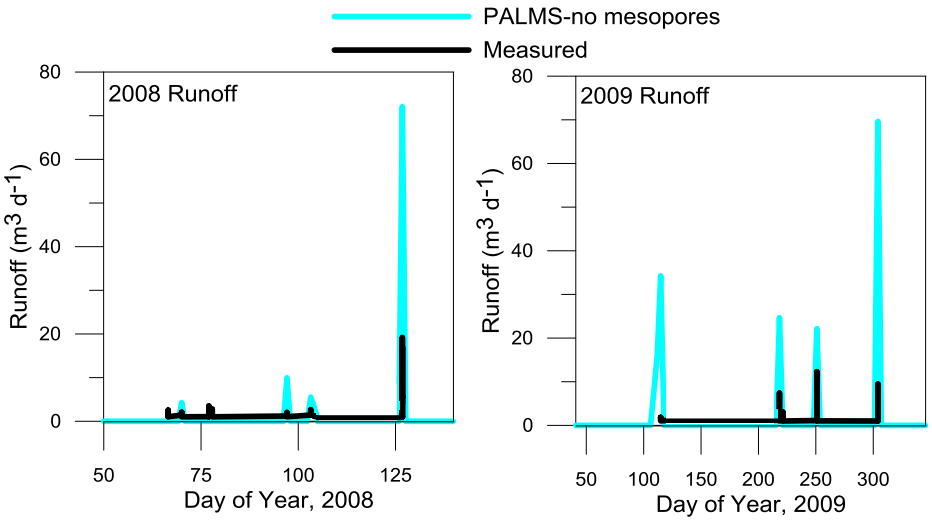

Figure 3.15. Runoff predicted by PALMS without mesopores compared to measured runoff on field SW17 at Riesel, TX for portions of 2008 and 2009. No runoff was modeled by PALMS with mesopores.

Soil VWC profiles from the NMM and PALMS with M&M on and off are plotted for four days on SW17 in 2009 (Fig. 3.16). The NMM readings were timed after a rainfall and depict wetting soil. By consulting the plots of yearly VWC for 2009 (Fig. 3.13), it is seen that the wetting event in May (Fig. 3.16 A) occurred with soil water content above 0.35 m^3 m^{-3}. The soil profile wets up more quickly and agrees more closely with the NMM measurements when the M&M module is used. After a rainfall event on drier soil on July 5th (Fig. 3.16 B), PALMS with and without the M&M module over predict water at the surface, but the M&M module is able to route water to depth and better represents the activity measured in the field. After both rainfall events in October (Fig. 3.16 C and D) it is seen that the wetter soil predicted by the M&M module

agrees more closely with the NMM measurements than does PALMS without the M&M module.

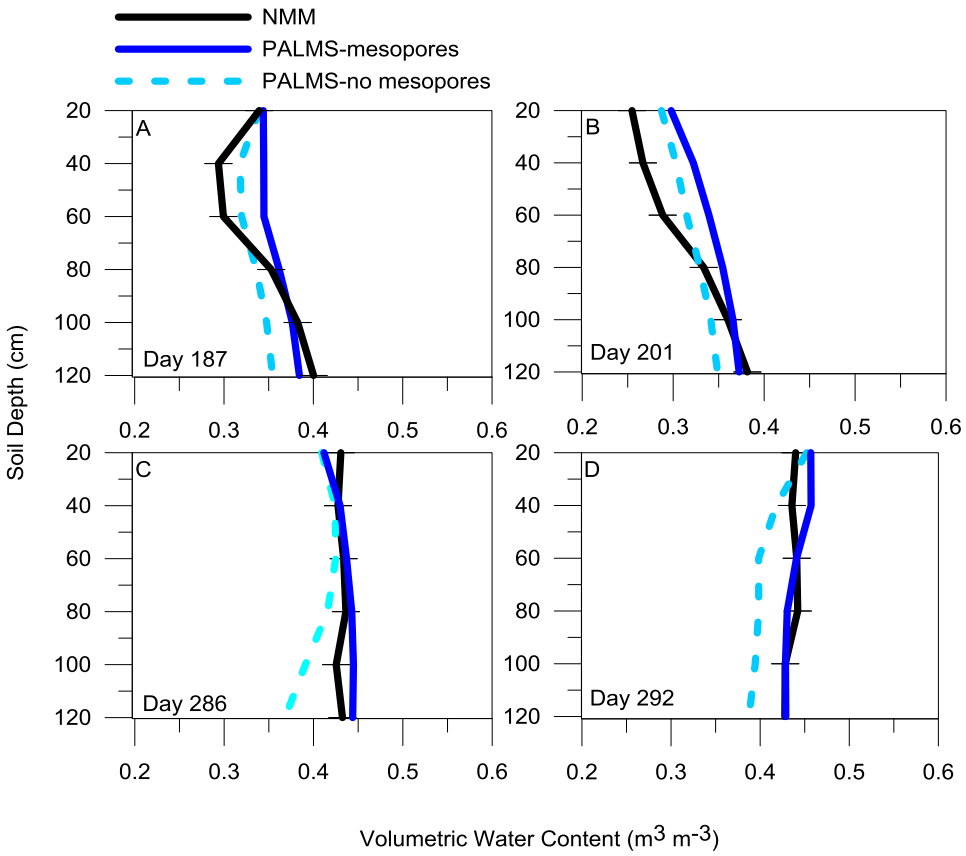

Figure 3.16. Volumetric water content with depth for PALMS and neutron moisture meter (NMM) for selected days on field SW17 at Riesel, TX. Shown are May 23rd (A), July 5th (B), October 12th, and October 18th of 2009.

Overall, the M&M module allowed the modeled soil profile to wet more deeply, generally improving estimates of VWC at the plot and field scales. Using the M&M module removed unobserved ponding at the plot scale and runoff events as much as six times too large at the field scale. The removal of runoff events came at the cost of what is likely excessive drainage.

CHAPTER IV

CONCLUSIONS

Three research questions were posed in this project: 1) how does the area of mesopores generated by the PALMS M&M module compare to measurements of crack area, 2) what is the influence of COLE values on preferential flow path volume in the PALMS M&M module, and 3) how well does the PALMS M&M module represent water flow on a cracked Texas soil under intense rainfall? Field investigations, analysis of previously collect cracking, runoff, and volumetric water content (VWC) data, and comparison of PALMS module simulations has lead us to the following conclusions.

On cracked soil irrigated at the plot scale, dry initial conditions translated to faster moving wetting fronts, presumably because crack networks were deeper. When 22 mm of water was applied to a dry plot in 1 hr., the wetting front in all soil measurements had reached 120 cm when measurements were taken 1.5 hrs after irrigation began. For the same amount and intensity of rainfall, wetter initial soil water contents had shallower wetting fronts. When irrigation was applied to soil at lower water contents, the variability in wetting front depth and soil moisture was higher among neutron moisture meter (NMM) access tubes than soils with higher water content—likely due to cracking networks. The greatest variability among NMM access tubes was seen after cracked soils were irrigated, during the period before water had fully redistributed in the soil profile. The measurements suggest that the time needed for free water to have drained from cracks and mesopores is between 24 and 72 hours.

Between the start of infiltration and the end of drainage of free water from soil cracks and mesopores, the free water in these spaces influences the count ratio taken by the NMM. A field study found free water surrounding the NMM access tube to influence volumetric water content to a lesser degree than predicted by a theoretical model (Crespo, 2014). Unlike the annuluses used in the field study by Crespo (2014), it is doubtful that cracks are totally filled with water (air gaps will reduce the count ratio, countering the water filled voids) or that they completely surround the access tubes. The uncertainty due to water filled cracks found in the field study was roughly half of the highest standard deviation among access tubes on both of the 10-by-10-m plots used in this study. While water retained in cracks and mesopores after the irrigation events was clearly a source of uncertainty in the NMM measurements, it still provided useful information regarding how long the water stays in the cracks and soil water redistribution. At the plot scale, the author found variability between access tubes to be similar to the uncertainty introduced by water in soil cracks, while the water in the soil cracks created a clear bias.

The M&M module in PALMS generates a mesopore volume that is linearly related to, and roughly ten times as large as the crack volume measured by infilling cracks with cement. However, the M&M module accounts for shrinkage that is not restricted to cracks that conduct cement. The M&M module also accounts for inter-pedal shrinkage. M&M module mesopore volume was sufficient to accommodate both the highest intensity (22 mm hr^{-1}) and the greatest volume of water applied (66 mm) without ponding at any time. In the drier of the two 66 mm irrigation events, no ponding was

observed. In the irrigation that was initially wetter, water ponded after 56 mm had been applied. Differing COLE values within the reasonable range of clay soils did not have a significant impact on modeled volumetric water content, infiltration, or change in macropore slit width.

PALMS with the M&M module wet the soil profile comparably to PALMS without the M&M module in the high intensity irrigation event on dry soil. The primary difference was that the M&M module drained the water and the Richards' equation did not allow the water to infiltrate, so it ran off. Soil water content profiles from all other irrigation events suggest that the M&M module performed better (VWC profiles were more like that of the NMM). The M&M module performed the best when irrigation times were longer and irrigation intensity was lower. When cracks are present in the soil profile, PALMS is improved when the M&M module is used because it creates a deeper wetting front than PALMS otherwise would. In broad terms, the M&M module drains the portion of the water that PALMS would otherwise pond. The differences in ponding, drainage, and wetting front depth between the PALMS with and without the M&M module are most clearly seen within 24 hours of the start of irrigation.

Three simulations that lasted a year and used topography and weather data from a 4.4 ha Vertisol field in Riesel, TX resulted in slight differences between using or not using the M&M module. Measurements of soil profile VWC and runoff in this field were compared to simulated VWC and runoff by PALMS with and without the M&M module. The faster moving wetting front that the M&M module produced becomes more apparent with depth. Use of the M&M module in PALMS roughly doubles the drainage

while eliminating ponding and therefore runoff. While not using the M&M module in PALMS overestimated runoff by as much as six times that of the measured values.

Usefulness of the M&M Module on Cracking Vertisol Landscapes

The criteria the given for a model that could be used on a shrink-swell soil landscapes that form cracks were that it 1) represent flow through a heterogeneous system, 2) have practically obtainable parameters at the landscape scale, and 3) allow for dynamic volume of cracks. The author has assessed how well the M&M module meets these criteria.

1) The PALMS M&M module meets the first criteria in that water does not need to saturate a soil layer before moving to the next soil layer, thus by-bass flow is achieved. The M&M module transports water to depth faster than the NMM measurements show water moving in the field. When irrigation water was applied over one hour, the NMM saw water draining for at least 24 hours afterwards, while the M&M module predicted that drainage would be over within 15 minutes of the end of irrigation. Either retaining the water artificially so that it had a longer time in which to infiltrate soil peds or increasing hydraulic conductivity could result in M&M module predictions that more closely resemble measured water contents. The issue with either of these approaches in this work is that there is not a good understanding of how this time or hydraulic conductivity adjustment should change across a landscape and so introducing them would currently disqualify the model for criteria 2.

2) The M&M module has practically obtainable parameters at the landscape scale. The nine parameters required were found using the soil survey information available through the NRCS official soil series descriptions (the Field Book for Describing and Sampling Soils was used for interpretations) and in the Rawls (1992) look-up tables, which are used as PALMS defaults.
3) The PALMS M&M module does not practically meet the third criteria because, though it has a dynamic volume of preferential flow path space, the volume is so great that changes in COLE values for the M&M module have no practical effect on infiltration. Any reasonable COLE value (0.01 to 0.17 $m^3\ m^{-3}$) would result in as much or more bypass flow than what is observed in the field. The presence or absence of the M&M module is more critical than a precise COLE value. Reducing COLE values below the reasonable range for a clay might narrow mesopores to a degree that they matched cement-filled crack volumes, but the current low hydraulic conductivity and quick moving wetting front are greater concerns for improvement than better representation of cracking.

The M&M module has fewer parameters than many two-domain models and a key advantage of the M&M module over other two-domain models is that the parameters have physical meaning and are easily obtainable. The M&M module within PALMS is a practical choice for modeling water flow on watersheds dominated by shrink-swell clays. Doing so will avoid the unreasonably high volumes of runoff that PALMS will otherwise predict, but sacrifices the generation of any runoff events. The author expects

the M&M module to predict volumetric water contents similar to or more accurate than PALMS otherwise would, with better predictions at depth than PALMS without the M&M module. PALMS with the M&M module is likely to predict more drainage.

Recommendations

Developing a recommendation on how to improve the experimental design of this experiment is difficult. The major problems with comparing measured to simulated results revolved around having free water in soil cracks. Using another measurement technique, such as time domain reflectrometry would have had limitations in the same measurement environment. The lack of drainage measurements in either field study made it difficult to know if the predicted drainage fell within a reasonable range. Future work could compare M&M module predictions to measurements of runoff, volumetric water content, and drainage to obtain a more complete picture of the fate of water in the soil profile. However measuring soil drainage in a Vertisol has technical complications as well. In the literature on modeling preferential flow of water through high clay soils there is a complete dearth of data sets for validation. Regarding the actual M&M model in PALMS, drainage is likely too high and the soil needs more time to absorb the free water being held in soil cracks. Currently, the M&M model drains this water. Additionally, the PALMS M&M module should allow for mesopores to close more completely after sufficient wetting.

REFERENCES

Ahuja, L.R., D.G DeCoursey, B.B. Barnes, and K.W. Rojas. 1993. Characteristics of macropore transport studied with the ARS root zone water quality model. Am. Soc. Ag. En. J. 36:369-380.

Arnold, J.G., K.N. Potter, K.W. King, and P.M. Allen. 2005. Estimation of soil cracking and the effect on surface runoff in a Texas Blackland Prairie watershed. Hydrol. Proc.19:589-603.

Beven, K.J., and P. Germann. 1982. Macropores and water flow in soils. Water Resour. Res. 18:1311-1325.

Beven, K.J., and R.T. Clarke. 1986. On the variation of infiltration into a homogenous soil matrix containing a population of macropores. Water Resour. Res. 22: 383-388.

Bird, R.B., W.E. Stewart, and E.N. Lightfoot. 1960. Transport Phenomena. New York: John Wiley and Sons.

Bouma, J.1980. Field measurement of soil hydraulic properties characterizing water movement through sourlling clay soils. J Hydrol. 45:149-158.

Bouma, J., and P. De Laat. 1980. Estimation of the moisture supply capacity of some swelling clay soils in the Netherlands. J. Hydrol. 49: 247-259.

Bouma, J., and L.W. Dekker . 1978. A case study on infiltration into dry clay soil I. Morphalogical observations. Geoderma 20:27-40.

Bronswijk, J.J.B. 1989. Prediction of actual cracking and subsidence in clay soils. Soil Sci. Soc. Am. J.148:87-93.

Chen, C., D.M. Thomas, R.E. Green, and R.J. Wagenet. 1993. Two-domain estimation of hydraulic properties in macropore soils. Soil Sci. Soc. Am. J. 57:680-686.

Connonlly, R.D. 1998. Modelling effects of soil structure on water balance of soil-crop systems: a review. Soil Till. Res. 48:1-19

Crespo, P.M. 2014. Field experiment on the effect of an air and water-filled annulus around a neutron access tube. Masters thesis, Eidgenössische Technische Hochschule Zürich.

Dasog, G.S., and G.B. Shashidhara. 1993. Dimension and volume of cracks in a Vertisol under different crop covers. Soil Sci. Soc. Am. J.6:424-428.

Delta-T Devices Ltd. 2005. User manual for the moisture meter type HH2. Version 4. Cambridge, UK. Burwell.

Dinka, T.A, C.L.S. Morgan, K.J. McInnes, A. S. Kishné, and R.D. Harmel. 2012. Shrink-swell behavior of soil across a vertisol catena. J. Hydrol. 476:352-359.

Fityus, S., T.Wells, and W. Huang. 2011. Water content measurement in expansive soils. Geotech. Test. J. 34:1-10.

Gerke, H.H., and J.M. Köhne. 2002. Estimating hydraulic properties of soil aggregate skins from sorptivity and water retention. Soil Sci. Soc. Am. J. 66:26-36

Greve, A., M.S. Anderson, and R.I. Acworth. 2010. Investigations of soil cracking and preferential flow in a weighing lysimeter filled with cracking clay soil. J. Hydrol. 393:105-113.

Harmel, R., C. Richardson, K. King, and P. Allen. 2006. Runoff and soil loss relationships for the Texas Blackland Prairies ecoregion. Geoderma 331:471-483.

ICT International, Pty Ltd. Neutron Probe Operation Manual. Retrieved November 11, 2013, from http://www.ictinternational.com.au/brochures/503drmanual.pdf

Jarvis, N.J., and P. Leeds-Harrison. 1990. Field test of water balance model of cracking clay soils. J. Hydrol. 112:203-218.

Jarvis, N.J. 2008. Near-saturated hydraulic properties of macroporous soils. Vadose Zone J. 7:1302-1310.

Jury, W.A., W.R Gardener, and W.H. Gardener. 1991. Soil Physics, fifth edition. John Wiley and Sons, New York. Page123.

Kishné, A.Sz., C.L.S. Morgan, and W.L. Miller. 2009. Vertisol crack extent associated with gilgai and soil moisture in the Texas Gulf Coast prairie. Soil Sci. Soc. Am. J. 73:1221-1230.

Kishné, A. Sz., C.L.S Morgan, Y. Ge, and W. Miller. 2010. Antecedent soil moisture affecting surface cracking of a vertisol in field conditions. Geoderma. 157:109-117.

Kroes, J.G., J.C. Wesseling, J.C. Van Dam. 2000. Integrated modelling of the soil-water-atmosphere-plant system using the model SWAP 2.0 an overview of the theory and an application. Hydrol. Proc. 14:1993-2002.

Larsson, M.H, and N.J. Jarvis. 1999. Evaluation of a dual-porosity model to predict field-scale solute transport in macroporous soil. J. Hydrol. 215:153-171.

Lepore, B.J., C.L.S. Morgan, J. M. Norman, and C.C. Molling. 2009. A mesopore and matrix infiltration model based on soil structure. Geoderma 152:301-313.

Luxmoore, R.J, P.M. Jardine, G.V. Wilson, J.R. Jones, L.W. Zelanzy. 1990. Physical and chemical controls of preferred path flow through a forested hillslope. Geoderma 46:139-154.

Li, J., D.W. Smith, and S.G. Fityus. 2003. The effect of a gap between the access tube and the soil during neutron probe measurements. Australian J. Soil Res. 41:151-164.

Ma, L., L.R. Ahuja, B.T. Nolan, R.W. Malone, T.J, Trout, Z. Qi. 2012. Root zone water quality model (RZWQM2): model use, calibration, and validation. Trans. ASABE. 5: 1425-1446

McBratney, A.B., B. Minasny, S.R. Cattle, and R.W. Vervoort. 2002. From pedotransfer functions to soil inference systems. Geoderma 109:41-73.

Microsoft. (2013). Microsoft excel computer software. Redmond, Washington: Microsoft.

Morgan, C.L.S. 2003. Quantifying soil morphological properties for landscape scale management applications. University of Wisconsin, Madison.

National Cooperative Soil Survey. National cooperative soil characterization database. Available online at http://ncsslabdatamart.sc.egov.usda.gov. Date accessed: 2/28/2014 12:11:41 PM

National Resource Conservation Service. Calculated coefficients of linear extensibility for 20-69% clay. Available online at www.nrcs.usda.gov/wps/portal/nrcs/detail/soils/survey /office/ssr10/tr/?cid=nrcs144p2_074840. Date accessed: 4/21/2014 9:34:11 AM

National Soil Survey Center. 2002. Field book for describing and sampling soils. Version 2.0. U.S. department of agriculture. Lincoln, Nebraska.

Neely, H.L., J.P. Ackerson, C.L.S. Morgan, and K.J. McInnes. 2014. Instrumentation to measure soil subsidence and water content in a single borehole. Soil Sci. Soc. Am. J. 48:4

Neely, H.L. 2014. Spatial and temporal distribution of dessication cracks in shrink-swell soils. Texas A&M University.

Nimmo, J.R. 2010. Theory for source-responsive and free-surface film modeling of unsaturated flow. Vadose Zone J. 12:295-306.

Nimmo, J.R. and L. Mitchell. 2013. Predicting vertically nonsequential wetting patterns with a source-responsive model. Vadose Zone J. 9 1-11.

Novák, V., J. Šimůnek, and M. TH. van Genuchten. 2000. Infiltration of water into soil with cracks. J. Irrig. Drain. En. 126:41-47.

Peng, X., R. Horn, S. Peth, and A. Smucker. 2006. Quantification of soil shrinkage in 2D by digital image processing of soil surface. Soil Till. Res. 91:173-180.

Porter, M.A, and T.A. McMahon. 1990. MUTillS-The Melbourne University tilled soil model. Am. Soc. Ag. En. J. 33:419-431.

Rawls, W.J., D.L. Brakensiek, K.E. Saxton. 1992. Estimation of soil water properties. Trans. ASABE. 25:1316-120 & 1328.

Richards, L.A. 1931. Capillary conduction of liquids through porous mediums. Physics. 1:318-333.

Ritchie, J.T. 1972. Model for predicting evaporation from row crop with incomplete cover. Water Resour. Res. 8:1204-1213

Rivera, L.D. 2011. Comparing methods of estimating crack volume in shrink-swell soils. Thesis, Texas A&M University. Available electronically from http://repository.tamu.edu/handle/1969.1/98359.

Šimůnek, J., N.J. Jarvis , M. TH. van Genuchten, and A. Gärdenäs. 2003. Review and comparison of models for describing non-equilibrium and preferential flow and transport in the vadose zone. J Hydrol. 272:14-35.

Topp, G., and J. Davis. 1981. Detecting infiltration of water through soil cracks by time-domain reflectometry. Geoderma 26:13-23.

USDA ARS. 2014. Pubilically avaible data. United states department of agriculture agricultural research station at riesel. Accesssed on 06/01/2014. http://www.ars.usda.gov/Research/docs.htm?docid=9699

van Schaik, N.L.M.B., R.F.A. Henriks, and J.C. van Dam. 2010. Parameterization of macropore flow using dye-tracer infiltration patterns in the SWAP model. Vadose Zone J. 9:95-106.

Wang, D., J.M. Norman, B. Lowery, and K. McSweeney. 1994. Nondestructive determination of hydrogeometrical characteristics of soil macropores. Soil Sci. Soc. Am. J. 58:294-303.

Wu, L., J.A. Vomocil, S.W. Childs. 1990. Pore size, particle size, aggregate size, and water retention. Soil Sci. Soc. Am. J. 54:952-956.

Yassoglou, N., C.S. Kosmas, N. Moustakas, E. Tzianis, and N.G. Danalatos. 1994. Cracking in recent alluvial soils as related to easily determined soil properties. Geoderma. 63:289-298.